J|A|C|S
ARTICLES
Published on Web 02/06/2003

Theoretical Conformational Analysis for Neurotransmitters in the Gas Phase and in Aqueous Solution. Norepinephrine

Peter I. Nagy,*,† Giuliano Alagona,*,‡ Caterina Ghio,‡ and Krisztina Takács-Novák§

Contribution from the Department of Medicinal and Biological Chemistry, The University of Toledo, Toledo, Ohio 43606-3390, Institute for Physical Chemistry Processes, Molecular Modeling Lab, CNR-IPCF, Via Moruzzi 1, I-56124 Pisa, Italy, and Institute of Pharmaceutical Chemistry, Semmelweis University, Högyes E. u. 9, H-1092 Budapest, Hungary

Received October 15, 2002; E-mail: pnagy@utnet.utoledo.edu; G.Alagona@icqem.pi.cnr.it

Abstract: The natural neurotransmitter (*R*)-norepinephrine takes the monocationic form in 93% abundance at the physiological tissue pH of 7.4. Ab initio and DFT/B3LYP calculations were performed for 12 protonated conformers of (*R*)-norepinephrine in the gas phase with geometry optimizations up to the MP2/6-311++G** level, and with single-point calculations up to the QCISD(T) level at the HF/6-31G*-optimized geometries. Four monohydrates were studied at the MP2/6-31G*//HF/6-31G* level. In the gas phase, the G1 conformer is the most stable with phenyl···NH_3^+ gauche and HO(alc)···NH_3^+ gauche arrangements. A strained intramolecular hydrogen bond was found for conformers (G1 and T) with close NH_3^+ and OH groups. Upon rotation of the NH_3^+ group as a whole unit about the $C_\beta-C_\alpha$ axis, a 3-fold potential was calculated with free energies for barriers of 3−12 kcal/mol at the HF/6-31G* level. Only small deviations were found in MP2/6-311++G** single-point calculations. A 2-fold potential was calculated for the phenyl rotation with free energies of 11−13 kcal/mol for the barriers at $T = 310$ K and $p = 1$ atm. A molecular mechanics docking study of (*R*)-norepinephrine in a model binding pocket of the β-adrenergic receptor shows that the ligand takes a conformation close to the T(3) arrangement. The effect of aqueous solvation was considered by the free energy perturbation method implemented in Monte Carlo simulations. There are 4−5 strongly bound water molecules in hydrogen bonds to the conformers. Although hydration stabilizes mostly the G2 form with gauche phenyl···NH_3^+ arrangement and a water-exposed NH_3^+ group, the conformer population becomes T > G1 > G2, in agreement with the PMR spectroscopy measurements by Solmajer et al. (*Z. Naturforsch.* **1983**, *38c*, 758). Solvent effects reduce the free energies for barriers to 3−6 and 9−12 kcal/mol for rotations about the $C_\beta-C_\alpha$ and the C_1(ring)$-C_\beta$ axes, respectively.

I. Introduction

Neurotransmitters are small molecules with prominent biological importance. Norepinephrine, epinephrine, serotonin, and dopamine have neurotransmitter function in the human organism.[1] In the adrenergic neurons of the vegetative nervous system, which maintains the normal homeostasis of the body, mainly norepinephrine is responsible for the neurotransmission. This molecule is synthesized starting from tyrosine, and is stored in the vesicles of the presynaptic region of the neuromuscular junction. By the impact of impulse it is released with exocytosis to the synaptic cleft, and is transported by passive diffusion to the postsynaptic membrane, where it activates α- and β-adrenergic receptors. This leads to the propagation of a nerve impulse. The therapeutic importance of norepinephrine is associated with its strong vasopressor activity, and is used to increase blood pressure in shock and vasomotor collapse. Epinephrine is the primary hormone secreted by the adrenal medulla. It plays a fundamental role in stress reactions. Serotonin and dopamine are also neurotransmitters acting predominantly in the central nervous system (CNS), but serotonergic and dopaminergic nerve endings have been identified elsewhere in the periphery. Histamine, another important endogenous amine, has a key function in allergic responses.

Ephedrine and norephedrine are sympathomimetic drugs used primarily as nasal vasoconstrictors for local application. Amphetamine and its methyl derivative show psychostimulant activity. Their therapeutic use is marginal; conversely, they are among the most frequently utilized narcotic agents in drug abuse.

All molecules above can be considered as substituted ethanes (Chart 1). One of the substituents is an amino group (methylated for structures **4**, **6**, and **9**) on C_α; another substituent is an aromatic ring on the C_β atom. The conformational freedom can be primarily characterized by rotations about the $C_\beta-C_\alpha$ and C_1-C_β single bonds.

The bioactive form of ligands, that is, the conformation taken

* Address correspondence to these authors. (P.I.N.) Phone: (419) 530-1945. Fax: (419) 530-7946. (G.A.) Phone: +39-050-3152450. Fax: +39-050-3152442.
† The University of Toledo.
‡ CNR-IPCF.
§ Semmelweis University.

(1) (a) Goodman & Gilman's *The Pharmacological Basis of Therapeutics*, 9th ed.; Hardman, J. G., Limbird, L. E., Molinoff, P. B., Goodman Gilman, A., Eds.; McGraw-Hill: New York, 1996. (b) Foye's *Principles of Medicinal Chemistry*, 5th ed.; Williams, D. A., Lemke, T. L., Eds.; Lippincott, Williams & Wilkins: Baltimore, MD, 2002.

10.1021/ja028952n CCC: $25.00 © 2003 American Chemical Society

Chart 1. 1−6, One Protonation Site (Monoamines), 7−10, Two Protonation Sites (Ampholytes), and 11, Two Protonation Sites (Bivalent Base)

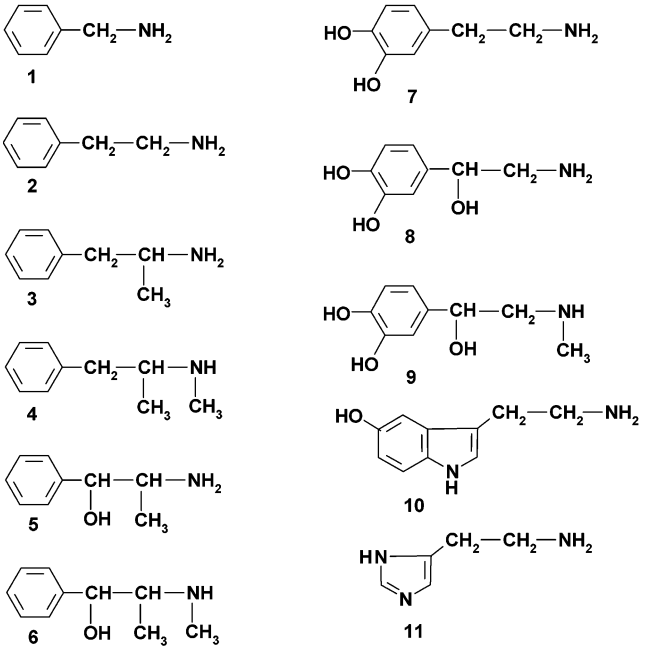

when the ligand is bound to the receptor and activates it, may easily differ from the most stable unbound structure. A free energy increase for this distortion can only be covered by a free energy decrease due to intermolecular interactions and subsequent changes in the chemical environment. Knowledge of the rotational potential for a ligand helps estimate the necessary minimum for a free energy decrease upon the formation of the ligand−receptor complex. Theoretical values are even more important in cases such as norepinephrine and its receptors, where no experimental information is available regarding the structure of the bioactive complex.

The proper designation of the protonation state for neurotransmitters in aqueous solution is a prerequisite for their structural characterization. According to the widely accepted concept,[1] a ligand binds to the receptor in a protonation state that the ligand took in aqueous solution at the physiological tissue pH 7.4. Exploration of the prevailing protonation state of molecules in Chart 1 must be based on consideration of the equilibrium mixture of differently protonated species. Table 1 contains the first and second protonation macroconstants for molecules with one or two protonation sites, structures **1**−**6** and **7**−**11**, respectively. As will be discussed later, each molecule has the cationic form as the predominant protonation state at pH 7.4. Thus, the subject of the present study is a theoretical conformational analysis for protonated norepinephrine (structure **8** in Chart 1) in the gas phase and in aqueous solution. The present study is a continuation of our recent modeling work in the field of neurotransmitter structure analysis in solution for histamine,[2] dopamine and its analogues,[3] and γ-aminobutyric acid.[4] A study for serotonin is planned for the near future.

Chart 2[a]

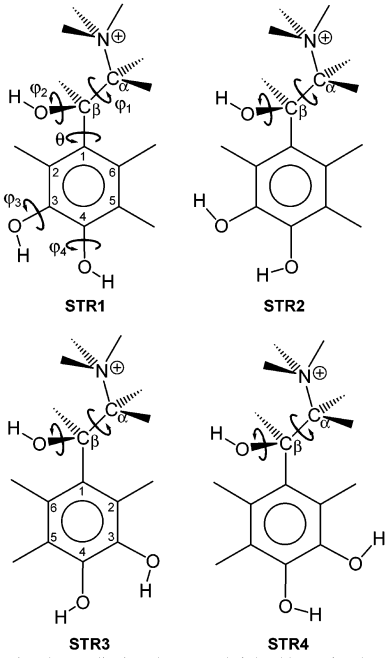

[a] The main rotatable bonds are displayed on the upper left backbone for the trans ($C_1C_\beta C_\alpha N = 180°$) position of the side chain. For STR1 and STR3 the ring atom numbering is also shown. Counterclockwise rotations of $-NH_3^+$ about $C_\alpha-C_\beta$ (looking from C_α) and of the phenyl ring, with $\theta = C_6C_1C_\beta C_\alpha$, about the C_1-C_β axis (looking from C_1) are positive. θ is equal to 0° in STR1/STR2 and to 180° in STR3/STR4. In STR1/STR3 $\varphi_3 = \varphi_4 = 0°$, while in STR2/STR4 $\varphi_3 = \varphi_4 = 180°$. Trans and gauche conformers, T, G1, and G2, can be obtained by flexible rotation about the $C_\alpha-C_\beta$ axis. Therefore, the optimized values for STR1−4, indicated with the (1)−(4) extensions of the T, G1, and G2 conformer names, only roughly correspond to the arrangements displayed.

II. Methods

Experiments. The standard potentiometric method (temperature 25.0 ± 0.1 °C, ionic strength 0.1 M, N_2 atmosphere) was used for the determination of the protonation macroconstants of the samples.[5] UV/pH titration was applied to obtain the protonation microconstant (log $k_1°$) of serotonin.[6] The theory, calculations, experimental details, and instruments (PCA 101 pK_a and log P analyzer, Sirius Ltd., Forest Row, U.K., and Hewlett-Packard 8452A diode-array spectrometer) used have been described previously.[6,7] Three separate measurements were carried out, and the average pK_a values along with the standard deviations were calculated (Table 1).

Calculations. Geometry optimizations for gas-phase conformers of protonated norepinephrine (Chart 2) were performed at the ab initio HF/6-31G*, MP2(FC)/6-31G*, HF/6-311++G**, and MP2(FC)/6-311++G** levels,[8] and at the DFT level by applying the B3LYP functional[9] (Table 2). The calculations were carried out using the Gaussian 98 software[10a] running in Pisa. Local energy minima were identified by frequency analysis at the HF/6-31G* level (Tables 3 and

(2) (a) Worth, G. A.; Richards, W. G. *J. Am. Chem. Soc.* **1994**, *116*, 239. (b) Nagy, P. I.; Durant, G. J.; Hoss, W. P.; Smith, D. A. *J. Am. Chem. Soc.* **1994**, *116*, 4898. (c) Karpinska, G.; Dobrowolski, J. C.; Mazurek. A. P. *J. Mol. Struct.: THEOCHEM* **1996**, *369*, 137. (d) Kovalainen, J. T.; Christiaans, J. A. M.; Ropponen, R.; Poso, A.; Perakyla, M.; Vepsalainen, J.; Laatikainen, R.; Gynther, J. *J. Am. Chem. Soc.* **2000**, *122*, 6989.

(3) (a) Urban, J. J.; Cramer, C. J.; Famini, G. R. *J. Am. Chem. Soc.* **1992**, *114*, 8226. (b) Urban, J. J.; Cronin, C. W.; Roberts, R. R. Famini, G. R. *J. Am. Chem. Soc.* **1997**, *119*, 12292. (c) Alagona, G.; Ghio, C. *Chem. Phys.* **1996**, *204*, 239. (d) Nagy, P. I.; Alagona, G.; Ghio, C. *J. Am. Chem. Soc.* **1999**, *121*, 4804. (e) Aliste, M. P.; Cassels, B. K. *J. Chem. Soc., Perkin Trans. 2* **2001**, 906.

(4) (a) Nagy, P. I.; Takács-Novák, K.; Ramek, M. *J. Phys. Chem. B* **2001**, *105*, 5772. (b) Ramek, M.; Nagy, P. I. *J. Phys. Chem. A* **2000**, *104*, 6844.

(5) Albert, A.; Serjeant, E. P. *The Determination of Ionization Constants*; Chapman and Hall: London, 1971.

(6) Takács-Novák, K.; Noszál, B.; Hermecz, I.; Keresztúri, G.; Podányi, B.; Szász, Gy. *J. Pharm. Sci.* **1990**, *79*, 1023.

(7) Nagy, P. I.; Takács-Novák, K. *J. Am. Chem. Soc.* **1997**, *119*, 4999.

(8) Hehre, W. J.; Radom, L.; Schleyer, P. v. R.; Pople, J. A. *Ab Initio Molecular Orbital Theory*; Wiley: New York, 1986.

4). Single-point calculations for these local-energy-minimum structures were performed at the MP2, MP3, MP4SDQ, QCISD, and QCISD-(T)[11] levels with the 6-31G* basis set (Table 5). Thermal corrections for obtaining standard relative internal free energies, $\Delta G°$(int), for the conformers at $T = 310$ K and $p = 1$ atm were calculated using the rigid rotator, harmonic oscillator approximation.[12] Accordingly, $\Delta G°$-(int) was calculated as

$$\Delta G°(\text{int}) = \Delta E + \Delta G_{\text{th}}(T) = \Delta E + \Delta\text{ZPE} + \Delta(H_{\text{vibr}}(T) - \text{ZPE}) - T\Delta S(T) \quad (1)$$

Here ΔE and $\Delta G_{\text{th}}(T)$ are the quantum chemically calculated internal energy difference and the so-called thermal correction, respectively. Contributions to the latter, ZPE, $H_{\text{vibr}}(T)$, and $S(T)$, are the zero-point energy, the vibration enthalpy, and the total entropy at T (=310 K), respectively.[13] For calculating the $\Delta G_{\text{th}}(T)$ term, two approximations were applied. In the first, the terms were calculated using the theoretical harmonic HF/6-31G* frequencies directly (unscaled values in Table 6). The method is known to overestimate the high frequencies relative to the experimental values by about 10%.[8,14] Pople et al. proposed a general scaling factor of 0.8953, and a scaling factor of 0.9135 for the ZPE term when HF/6-31G* calculations are performed.[14a] A scaling factor of 0.9061 was obtained by Scott and Radom[14b] when inverse experimental and HF/6-31G* frequencies were compared. The lowest theoretical frequencies for pyrrole and imidazole[15] are, however, overestimated by only 2−4% at about 500 cm^{-1} at this level, and the smallest calculated frequency for the predominant gas-phase conformer of 1,2-ethanediol[16] is *smaller* by about 10% than the lowest experimental value[17] of 212 cm^{-1}. In the second approach the lowest five frequencies for minima, and the lowest four for transition-state (TS) structures, all below or about 200 cm^{-1}, were left unscaled, and a scaling factor of 0.9 was applied for the remaining frequencies in ZPE (scaled results in Table 6). The frequencies starting from the sixth smallest one (fifth smallest one for TS structures) were also scaled in the thermal terms for $H_{\text{vibr}}(T)$ and $S_{\text{vibr}}(T)$, where the $h\nu$ energy term appears *out* of the exponent. Thus, for example, the sixth, seventh, etc. frequencies were scaled in the numerator, but not in the denominator, of the expressions $h\nu/(\exp(h\nu/kT) - 1)$ for $H_{\text{vibr}}(T)$ and $(h\nu/T)/(\exp(h\nu/kT) - 1)$ for S_{vibr}.[12] Frequencies appearing in the exponents were left unscaled everywhere. They produce the largest contribution to the thermal correction for the low-frequency motions (say, e.g., below 200 cm^{-1}). However, one expects just these frequencies to be underestimated at the HF/6-31G* level; thus, their values probably should be increased instead of decreased. Consequently, in the absence of a reliable scaling factor >1, these frequencies were kept unaltered. For larger frequencies the exponential terms increase rapidly or converge to 0 (in $\ln(1 - \exp(-h\nu/kT))$ for S_{vibr} and G_{vibr}) with or without a scaling factor of 0.9.

For the four protonated conformers of outstanding interest (see later) monohydrate structures were obtained by optimization at the HF/6-31G* level. Upon graphical assignment using the MOLDEN software,[10b] three water vibrations and six norepinephrine···water intermolecular vibrations were identified. Their contributions to ZPE, $H_{\text{vibr}}(T)$, and $S_{\text{vibr}}(T)$ were disregarded, and thermal corrections for the 24-atom protonated norepinephirine were calculated on the basis of the remaining 66 frequencies. The scaling procedure was taken as described above.

Relative conformational solvation free energies were obtained by using the free energy perturbation (FEP) method[18] as implemented in Monte Carlo (MC) simulations.[19] Calculations were carried out by the use of the BOSS 3.6 software[20] on a Silicon Graphics Indigo^2 workstation at the University of Toledo.

Monte Carlo simulations for the aqueous solution of protonated norepinephrine were performed in NpT (isobaric−isothermal) ensembles at $T = 310$ K and $p = 1$ atm.[21] A water box including 496 TIP4P water molecules[22] and a single solute were considered for the aqueous solution model. Solvation free energy changes were calculated for rotations about the $C_\beta-C_\alpha$ and C_1(ring)$-C_\beta$ axes. Geometries of the reference structures with changes of about 30° in the reaction path torsion angle were determined from gas-phase optimization at the HF/6-31G* level. Interaction energy of the solution elements was calculated using the 12−6−1 type OPLS pair potential.[23] Steric OPLS parameters were taken from the program library. For comparison with our previous results, we used the united-atom force field[23a] for exploring the solvent effect on group rotations. In this model, all solute atoms were considered explicitly except those in the CH and CH_2 groups, where the united-atom model was applied. To reduce the large computation time, rotational potentials were calculated for the gas-phase conformers using the united-atom force field. For the more subtle calculations of the conformational equilibrium, we used the all-atom force field.[23b] The solvent−solvent cutoff (RCUT) and the solute−solvent cutoff (SCUT) were set to 9.75 and 12 Å, respectively. Random translation and rotation for the solute were limited to 0.1 Å and 10°, respectively. Solute movement was attempted every 50 steps; volume alteration (with a maximum of 250 $Å^3$) was attempted every 1000 steps. Periodic boundary conditions and preferential sampling were applied with $c = 120$ in the sampling factor $1/(R^2 + c)$, where R is the distance between the C_1 ring atom and the central atom of the selected solvent molecule. With these simulation parameters, 40−50% of the newly generated configurations were accepted out of 3500K and 5000K configurations in the equilibrium and averaging phases, respectively.

If the 12−6−1 OPLS pair potential for calculation of the interaction energy is used, no polarization effects are considered explicitly. The TIP4P water model,[22] however, was optimized for producing good liquid properties (density and heat of vaporization); thus, the polarization

(9) (a) Lee, C.; Yang, W.; Parr, R. G. *Phys. Rev. B* **1988**, *37*, 785. (b) Becke, A. D. *J. Chem. Phys.* **1993**, *98*, 5648.

(10) (a) Gaussian 98, Revision A.6: Frisch, M. J.; Trucks, G. W.; Schlegel, H. B.; Scuseria, G. E.; Robb, M. A.; Cheeseman, J. R.; Zakrzewski, V. G.; Montgomery, J. A., Jr.; Stratmann, R. E.; Burant, J. C.; Dapprich, S.; Millam, J. M.; Daniels, A. D.; Kudin, K. N.; Strain, M. C.; Farkas, O.; Tomasi, J.; Barone, V.; Cossi, M.; Cammi, R.; Mennucci, B.; Pomelli, C.; Adamo, C.; Clifford, S.; Ochterski, J.; Petersson, G. A.; Ayala, P. Y.; Cui, Q.; Morokuma, K.; Malick, D. K.; Rabuck, A. D.; Raghavachari, K.; Foresman, J. B.; Cioslowski, J.; Ortiz, J. V.; Stefanov, B. B.; Liu, G.; Liashenko, A.; Piskorz, P.; Komaromi, I.; Gomperts, R.; Martin, R. L.; Fox, D. J.; Keith, T.; Al-Laham, M. A.; Peng, C. Y.; Nanayakkara, A.; Gonzalez, C.; Challacombe, M.; Gill, P. M. W.; Johnson, B.; Chen, W.; Wong, M. W.; Andres, J. L.; Gonzalez, C.; Head-Gordon, M.; Replogle, E. S.; Pople, J. A., Gaussian, Inc., Pittsburgh, PA, 1998. (b) MOLDEN 3.7: Schaftenaar, G., CMBI, The Netherlands (may be downloaded from http://www.cmbi.kun.nl/~schaft/molden/molden.html).

(11) Pople, J. A.; Head-Gordon, M.; Raghavachari, K. *J. Chem. Phys.* **1987**, *87*, 5968.

(12) McQuarrie, D. A. *Statistical Mechanics*; University Science Books: Sausalito, CA, 2000.

(13) Translational entropy has a term depending on the molar volume. If the standard state is changed, as in solution where the molar volume is 1 dm^3 corresponding to the unit chemical concentration, the $-TS(T)$ and $G°$(int) terms increase by $RT \ln V(T)$, where $V(T)$ is the molar volume in the gas phase at T. However, this term is additive and constant in $G°$(int) for conformers and thus will be canceled in $\Delta G°$(int).

(14) (a) Pople, J. A.; Scott, A. P.; Wong, M. W.; Radom, L. *Isr. J. Chem.* **1993**, *33*, 345. (b) Scott, A. P.; Radom, L. *J. Phys. Chem.* **1996**, *100*, 16502.

(15) Nagy, P. I.; Durant, G. J.; Smith, D. A. *J. Am. Chem. Soc.* **1993**, *115*, 2912.

(16) (a) Nagy, P. I.; Dunn, W. J., III; Alagona, G.; Ghio, C. *J. Am. Chem. Soc.* **1991**, *113*, 6719. (b) Nagy, P. I.; Dunn, W. J., III; Alagona, G.; Ghio, C. *J. Am. Chem. Soc.* **1992**, *114*, 4752. (c) Alagona, G.; Ghio, C. *J. Mol. Struct.: THEOCHEM* **1992**, *256*, 187.

(17) (a) Frei, H.; Ha, T.-K.; Meyer, R.; Gunthard, Hs. H. *Chem. Phys.* **1977**, *25*, 271. (b) Takeuchi, H.; Tasumi, M. *Chem. Phys.* **1983**, *77*, 21

(18) Zwanzig, *J. Chem. Phys.* **1954**, *22*, 1420.

(19) Jorgensen, W. L.; Ravimohan, C. *J. Chem. Phys.* **1985**, *83*, 3050.

(20) Jorgensen, W. L. BOSS, Version 3.6. *Biochemical and Organic Simulation System User's Manual*; Yale University: New Haven, CT, 1995.

(21) (a) Jorgensen, W. L.; Madura, J. D. *J. Am. Chem. Soc.* **1983**, *105*, 1407. (b) Jorgensen, W. L.; Swenson, C. J. *J. Am. Chem. Soc.* **1985**, *107*, 1489. (c) Jorgensen, W. L.; Gao, J. *J. Phys. Chem.* **1986**, *90*, 2174. (d) Jorgensen, W. L.; Briggs, J. M.; Contreras, M. L. *J. Phys. Chem.* **1990**, *94*, 1683.

(22) (a) Jorgensen, W. L.; Chandrasekhar, J.; Madura, J. D.; Impey, R. W.; Klein, M. L. *J. Chem. Phys.* **1983**, *79*, 926. (b) Jorgensen, W. L.; Madura, J. D. *Mol. Phys.* **1985**, *56*, 1381.

(23) (a) Jorgensen, W. L.; Tirado-Rives, J. *J. Am. Chem. Soc.* **1988**, *110*, 1657. (b) Jorgensen, W. L.; Maxwell, D. S.; Tirado-Rives, J. *J. Am. Chem. Soc.* **1996**, *118*, 11225.

effect is implicitly incorporated when the OPLS parameters are used. Mimicked polarized atomic charges can be obtained if the atomic charge parameters are fitted to the solute gas-phase HF/6-31G* molecular electrostatic potential. This is based on the finding that gas-phase HF/6-31G* dipole moments generally exceed experimental values by about 10−20%.[24] The solute atomic charges were derived in the present study by using the CHelpG procedure.[25] Charges were fitted to the reference structures (see above), i.e., for every structure with a change of about 30° in the $C_1C_\beta C_\alpha N$ and $C_6C_1C_\beta C_\alpha$ torsion angles (see Chart 2).

In FEP calculations, geometric and OPLS potential parameters for the perturbed systems are calculated as linear functions of the parameters for the reference structures at the ends of the path. In general, 10 perturbation steps were taken in an interval when the torsion angle changed by 30°. Using double-wide sampling, it means changes of about 1.5° in the selected reaction coordinate torsion angle. Converged results were reached by applying such small changes: calculating the rotation in the entire 360° range, the theoretical $\Delta G(\text{solv}) = 0$ value was well approached by 0.14 ± 0.30 and 0.31 ± 0.67 kcal/mol for the $C_1C_\beta C_\alpha N$ and $C_6C_1C_\beta C_\alpha$ rotations, respectively.

Long-range electrostatic (LRE) effects were obtained by using the polarizable continuum method (PCM).[26] The small calculated corrections were applied only for conformers considered in the in-solution equilibrium. With the ICUT = 2 option in BOSS 3.6, every solvent molecule is seen by the solute if it is within a sphere of $R = 12$ Å around any solute atom. Accordingly, the PCM energy was calculated for the conformers with a cavity formed by interlocking spheres around the solute atoms with $R = 12$ Å. The total conformational free energy difference was calculated as

$$\Delta G°(\text{total}) = \Delta G°(\text{int}) + \Delta G°(\text{solv}) \qquad (2)$$

where $\Delta G°$(int) is from eq 1, and $\Delta G°$(solv) is the relative solvation free energy for the conformers, as calculated by the FEP method and including LRE.

The general approach described above has two potential weaknesses. If the solute geometry differs remarkably from that optimized for the molecule in the absence of a chemical environment, then the applied geometry is not relevant in solution. As will be seen in the Results and Discussion, appropriate geometries distinct from those optimized in the gas phase have to be considered to properly characterize the conformational equilibrium. In T and G1 conformations (see Chart 2), the O and the H(N) atoms of the $HO-CH-CH_2-NH_3^+$ moiety are at distances of 2.1−2.3 Å, but the distance increases when the protonated amino group interacts with a water molecule. The monohydrate adduct provides a more adequate geometry for the protonated norepinephrine if its behavior in aqueous solution is to be studied. For comparisons on equal footing, T(1), G1(1), G2(1), and G2(3) monohydrate structures and energies were determined at the MP2/6-31G*//HF/6-31G* level.

The second problem in our approximation is that the electron distribution derived for protonated norepinephrine does not reflect the polarizing effect of the solvent. In the FEP calculations implemented in Monte Carlo simulations, the solute−solvent and solvent−solvent pair-interaction energies are supposed to account for interactions between polarized molecules. As was mentioned earlier in this section, the TIP4P model has effective charges that have been optimized to reproduce physical measurables for liquid water. Thus, these charges account implicitly for a proper water−water interaction-energy value. The largest problem in our approximation is to find the relevant solute charges.

There is seemingly a gap in the logic when gas-phase structural parameters are used for in-solution structures. For assigning effective charges, there are different methods. We used the approach of Orozco et al.[24b] to find the ELPO charges mimicking the polarized ones. In our former study for dopamine[3d] we compared the ELPO and CM2/AM1 charges[27,28] for several conformations of dopamine. It was found that the N atomic charges could differ by more than 0.3 units, although the $-NH_3^+$ group charges differed only by 0.01−0.06 charge units. In a study for the $ONOO^-$ anion,[29] the CM2/AM1 charges did not meet some qualitative requirements, whereas the CM2/PM3 charges[28,30] were fairly close to the ELPO ones. The CM2/PM3 parametrization, however, predicted an unjustifiably large stabilization of the cis conformer upon solvation, in contrast to all other methods in that study. In the present investigation we maintained the charge derivation from the HF/6-31G* molecular electrostatic potential. With this choice, we can compare the present results with those for dopamine, the structurally related neurotransmitter. A problem, however, still remains: if (effectively) polarized atomic charges are considered, then the internal energy should be calculated according to structures corresponding to this effective charge set. In fact, these structures should be considered to exist in solution.

Relative internal energies for in-solution polarized $ONOO^-$ conformers as compared to *relative* values for structures optimized in the gas phase differ by about 1 kcal at the top of the torsion barrier, but energies differ only by 0.01 kcal/mol for the local-energy-minimum structures.[29] The study suggests that both the energy shift following small changes in bond lengths and bond angles and the polarization effect upon solvation are nearly additive for stable conformers, and in-solution relevant energy and free energy *differences* can be satisfactorily established by using gas-phase structures and related ELPO charges. Nonetheless, the choice of the atomic charge set for the solute is a source of uncertainty for the present calculations.

As mentioned, equilibrium ratios for the T(1), G(1), G2(1), and G2-(3) conformers were calculated using their in-monohydrate geometries, and using the MP2/6-31G*//HF/6-31G* energies at that geometry. Relative solvation free energies were obtained in MC/FEP calculations by utilizing the all-atom OPLS-AA force field.[23b] First, the closest gas-phase geometry was transformed to the monohydrate geometry, using the OPLS-UA force field.[23a] Annihilation of the C−H hydrogens and development of the united CH and CH_2 atoms were performed along a nonphysical path using the AA and UA force field parameters at the two ends. An independent calculation for the phenyl rotation distinguishing G2(1) and G2(3) conformers was performed by using the OPLS-AA force field.

III. Results and Discussion

Basicity of Amines. Table 1 shows that, for all compounds in Chart 1, the prevailing structure is the monocationic form at pH 7.4. At least 93% of the species in the equilibrium mixtures take this protonation state. Thus, for an in-solution conformational analysis for the main component, the internal free energies are to be determined for protonated conformers in the gas phase, if the additivity of eq 2 is accepted.

For compounds **1**−**6**, the BH^+ form has a population of at least 98% at physiological pH. Comparison of the measured log K values highlights some trends related to the substituent effect and the importance of the length of the aliphatic spacer. Benzylamine (**1**) and phenylethylamine (**2**) differ by a $-CH_2-$ group. The $pK_a = \log K$ protonation constant, characterizing the basicity of the amine, increases by 0.4 units from compound **1** to compound **2**. Conversely, when methyl derivatives instead

(24) (a) Carlson, H. A.; Nguyen, T. B.; Orozco, M.; Jorgensen, W. L. *J. Comput. Chem.* **1993**, *14*, 1240. (b) Orozco, M.; Jorgensen, W. L.; Luque, F. J. *J. Comput. Chem.* **1993**, *14*, 1498.
(25) Breneman, C. M.; Wiberg, K. B. *J. Comput. Chem.* **1990**, *11*, 316.
(26) (a) Miertuš, S.; Scrocco, E.; Tomasi, J. *Chem. Phys.* **1981**, *55*, 117. (b) Miertuš, S.; Tomasi, J. *Chem. Phys.* **1982**, *65*, 239. (c) Tomasi, J.; Persico, M. *Chem. Rev.* **1994**, *94*, 2027.
(27) Li, J.; Zhu, T.; Cramer, C. J.; Truhlar, D. G. *J. Phys. Chem. A* **1998**, *102*, 1820.
(28) Dewar, M. J. S.; Zöbisch, E. G.; Healy, E. F.; Stewart, J. J. P. *J. Am. Chem. Soc.* **1988**, *110*, 1657.
(29) Nagy, P. I. *J. Phys. Chem. A* **2002**, *106*, 2659.
(30) Stewart, J. J. P. *J. Comput. Chem.* **1989**, *10*, 209.

Table 1. Protonation Macroconstants and Equilibrium Compositions at pH 7.4 and $T = 25$ °C

		distribution (%) of protonated species at pH 7.4	
compd[a]	log $K \pm$ SD	[B][b]	[BH$^+$][b]
1	9.43 ± 0.02	0.92	99.08
2	9.85 ± 0.01	0.35	99.65
3	9.96 ± 0.01	0.28	99.72
4	10.21 ± 0.01	0.15	99.85
5	9.11 ± 0.02	1.91	98.09
6	9.64 ± 0.01	0.57	99.43

			distribution (%) of protonated species at pH 7.4		
compd[a]	log $K_1 \pm$ SD	log $K_2 \pm$ SD	[X$^-$][c]	[XH][c]	[XH$_2^+$][c]
7	10.50 ± 0.01	8.92 ± 0.01	<0.01	2.93	97.06
8	9.63 ± 0.01	8.51 ± 0.01	0.04	7.20	92.76
9	9.96 ± 0.01	8.66 ± 0.01	0.01	5.20	94.78
10	10.90 ± 0.01	9.92 ± 0.01		0.30	99.70
11	9.80 ± 0.01	6.08 ± 0.01	0.37[d]	95.07[d]	4.55[d]

[a] For compound numbers, see Chart 1. [b] [B] and [BH$^+$] values refer to the percentage of the free and the protonated base, respectively. [c] [X$^-$], [XH], and [XH$_2^+$] values refer to the deprotonated, neutral, and protonated forms, respectively. [d] For histamine (compound **11**), the values refer to the B, BH$^+$, and BH$_2^{2+}$ neutral, monocationic, and dicationic forms, respectively.

of phenyl derivatives are considered, i.e., ethylamine and propylamine, their pK_a values are 10.65 and 10.54, respectively.[31a] This comparison suggests that the length of the spacer, $-CH_2-$ vs $-CH_2-CH_2-$, is much more important in the case of a phenyl substituent than in the case of a methyl substituent. The phenyl group itself causes a marked decrease in basicity, and the effect is larger when the spacer is shorter.

Secondary amines, compounds **4** and **6**, are stronger bases than their primary amine counterparts, **3** and **5**, respectively. Methyl substitution in the α position (**3** vs **2**) increases the basicity; OH substitution in the β position reduces the basicity (**5** vs **3**, **6** vs **4**). Although these general structure−property relationships might have been well-known for a long time, the present table providing data from a consistent methodology can be usefully applied for understanding log K_2 values for compounds **7**−**11** in the bottom part of Table 1.

log K values for compounds **7**−**11** are available from the literature, too.[31] Deviations from those values are generally no larger than about 0.1 units, with the exception of the serotonin log K_1 (compound **10**), where our value is lower by 0.2 units than that in ref 31a. The log K values presented in this paper have small standard deviations showing the large precision and reproducibility of the methodology applied.

In our former studies for histamine[2b] and dopamine,[3c,d] the monocationic form was thoroughly studied. Data in Table 1 confirm this choice. Also in the present study, the monocationic norepinephrine has been selected for a detailed analysis. Table 1 data for compounds **7**−**11** indicate, however, that other protonation states make up to 7% of the equilibrium mixture at physiological pH 7.4.

The X$^-$ anionic form stems from the deprotonation of an OH group for compounds **7**−**10**. The site is obvious for serotonin with a single phenolic OH. It is not clear for catechols (**7**−**9**), but the problem is beyond the scope of the present analysis. Nonetheless, the X$^-$ concentration is no more than 0.04% at the relevant pH, and can be disregarded with confidence.

More problematic is the second most populated form, the zero-net-charge structure. This form, XH, is a mixture of the so-called neutral form with NH_2 and OH groups, and the zwitterionic form with $-NH_3^+$ and $-O^-$ (phenolate) groups. Their *total* percentage is given in Table 1 without specification of their individual values. To obtain those latter percentages, the protonation microconstants should have been determined. Unfortunately, for compounds **7**−**9**, despite considerable efforts, the sensitivity of the catechol moiety to oxidation prevented the determination of the microconstants with acceptable reproducibility and low standard deviation (SD). In contrast, their determination for serotonin was successful in the absence of the technical problems met in the case of catechols. The serotonin values (for their definitions see, e.g., ref 7) are log $k_1° = 10.62 \pm 0.03$, log $k_1^{\pm} = 10.58$, log $k_2^{\pm} = 10.24$, and log $k_2° = 10.20$. The corresponding equilibrium mixture at pH 7.4 and $T = 25$ °C is 9.5×10^{-5}% anion, 0.13% zwitterion, 0.16% neutral, and 99.70% cation. By comparison with the data in Table 1, [zwitterion] + [neutral] = 0.29% as compared to the value of [XH] = 0.30%. The two values agree within the rounding error.

From the serotonin results, the zwitterionic and neutral forms are in nearly equal concentrations. This is not necessarily true in general, especially when applied to catechols where the two phenolic OH groups may form a hydrogen bond to each other. Consideration of this equilibrium is exciting, although it is not nearly as important as it was for the nicotinic acid isomers[7] and for the γ-aminobutyric acid (GABA).[4] For those systems, the zwitterionic form was the prevailing structure with a fraction of at least 95%. In contrast, data from Table 1 indicate that the monocationic form prevails for compounds **7**−**11**. For histamine (**11**), the monocationic form is present in 95.1% concentration. The second most populated form is the dication with a fraction of 4.6%, and the "least" protonated form is the free base with an equilibrium fraction of 0.4%.

What are the corresponding log K values for compounds **1**−**6** and **7**−**11**? For compounds **1**−**6**, log K is the equilibrium constant for the process B + H$^+$ ↔ BH$^+$. For compounds **7**−**10**, log K_1 is the macroconstant for the process X$^-$ (anion) + H$^+$ ↔ XH (zero net charge) where XH = zwitterion + neutral form. log K_2 refers to the protonation process XH + H$^+$ ↔ XH$_2^+$. Thus, since B and XH indicate net-zero-charge states, log K for compounds **1**−**6** is the counterpart of the log K_2 protonation macroconstant for compounds **7**−**10**. For histamine, log K_1 is the counterpart, because this macroconstant characterizes the B + H$^+$ ↔ BH$^+$ equilibrium.

Following the above assignment, the comparable macroconstants for catechol-type compounds **7**−**9** are smaller by about 0.6−1.0 log units than the related values for compounds **1**−**6**. log K and log K_2 for phenylethylamine (**2**) and dopamine (**7**) are 9.85 and 8.92, respectively. A similar decrease of log K has been found for norephedrine (**5**) and norepinephrine (**8**), from 9.11 to 8.51, and for ephedrine (**6**) and epinephrine (**9**), from 9.64 to 8.66. (There is an α-methyl group in compounds **5** and **6** as compared to **8** and **9**, but this effect may increase the basicity of compounds **5** and **6** by only about 0.1 log units, as extrapolated from the difference of the log K values for compounds **2** and **3**.) For histamine, log $K_1 = 9.80$ is close to the values for primary phenylethylamines without polar substituents (**2** and **3**). The serotonin log K_2 equals 9.92, and the

(31) (a) *CRC Handbook of Chemistry and Physics*, 83rd ed; CRC Press LLC: Boca Raton, FL, 2002 (b) Martin, R. B. *J. Phys. Chem.* **1971**, *75*, 2657.

protonation microconstant for the neutral form, log $k_2° = 10.20$, is even *larger* than the macroconstant, log $K = 9.85$, for phenylethylamine. The larger log $k_2°$, characterizing the $-NH_2 + H^+ \leftrightarrow -NH_3^+$ equilibrium, indicates the increased basicity of neutral serotonin. Thus, replacement of the phenyl group by an imidazole (histamine) or by an indole group (even having a 5-OH substituent for serotonin) results in a negligible change for the macroconstant, but the 3,4-dihydroxy substitution of the phenyl ring reduces log K_2 considerably as compared to log K for compounds **2** and **3**.

Recently several papers have been published on the neutral form of 1-amino-2-phenylethane derivatives and their water complexes in the gas phase. Alagona and Ghio, besides the protonated form, studied neutral norepinephrine and its monohydrate.[32] Structures and hydrates for molecules without 3,4-dihydroxy substituents, such as 2-phenylethylamine,[33a] 2-amino-1-phenylethanol,[33b] ephedrine and pseudoephedrine,[33c] and *p*-methoxyphenethylamine,[33d] have been studied by different research groups. Common in these studies is that the neutral form was considered, which corresponds to a gas-phase structure. Although Table 1 shows that these types of molecules take mostly the protonated form in aqueous solution, the above studies can provide good starting points to the structure analysis of neutral dopamine and norepinephrine that are also present in 3−7% concentration.

Norepinephrine. Geometry and Intramolecular Hydrogen Bonds. The conformation of the catechol part was recently studied in detail by Alagona and Ghio.[32] It was pointed out that local-minimum-energy structures on the HF/6-31G* potential energy surface correspond to conformations where the vicinal phenolic OH groups form practically planar five-membered rings. The arrangements make possible the formation of intramolecular H−O···H−O hydrogen bonds with O···H distances of 2.17−2.19 Å and O−H···O angles of about 110°. These structures were accepted as low-energy conformations for the catechol ring, and were not further studied here (except in relation to the phenyl ring rotation).

Selected torsion angles (Chart 2) optimized at different levels and/or basis sets are compared in Table 2. The overall agreement of the data is good, and deviations are consistent. The torsion angles are always similar at the HF, B3LYP, and MP2 levels with the 6-31G* basis set. The only remarkable exception is the G2(1) $C_6C_1C_\beta C_\alpha$ torsion angle, where the HF value is larger by about 10° than the optimized B3LYP and MP2 ones. In other cases, torsion angles agree within a few degrees. MP2/6-311++G**-optimized values are consistently smaller than the other three for the G2 $C_1C_\beta C_\alpha N$ torsions, and are smaller and larger, respectively, for the G2(3) and T1(1) $C_6C_1C_\beta C_\alpha$ torsions. The deviations still do not exceed 10° in general. It may be concluded that the optimized torsion angles are similar, irrespective of the methods and basis sets used.

The alcoholic OH and the NH_3^+ groups are trans to each other in the G2 geometries, and they take a gauche relative position in the G1 and T conformers, as shown by the $OC_\beta C_\alpha N$ values in Table 2. Arrangements in G1 and T allow the formation of an O···H−N intramolecular hydrogen bond. The existence of such bonds has been studied for a long time. Since the early 1990s we have considered several 1,2-disubstituted ethane molecules: 1,2-ethanediol,[16] histamine,[2b] dopamine,[3c,d] and a restricted analogue, 2-hydroxybenzoic acid.[34] One of the main questions has always been whether intramolecular H-bonds, which are supposed to exist in some gas-phase conformations, are maintained after aqueous solvation. Hydrogen bonds were assigned for relatively short $R(X\cdots HY) < 2.4$ Å distances (X, Y = O, N) in the gas-phase-optimized structures, and upon shifts in the stretching frequencies for the Y−H bonds involved in the hypothesized intramolecular bonds.

In a recent analysis using the AIM method,[35] Klein did not find a bond critical point (BCP) along the O···H electron density in 1,2-ethanediol, and consequently no intramolecular H-bond was assumed in the tGg′ and gGg′ conformers.[36] Moreover, he did not find a BCP for any vicinal diols up to 1,2-hexanediol. It was concluded in that study that H···O distances of about 2.3 Å and O−H···O angles of about 110° for a five-membered ring including the O−C−C−O moiety and a H-atom from one of the alcoholic OH groups do not permit a hydrogen bond. Adding a water molecule to this conformer, the water oxygen mediates two intermolecular hydrogen bonds with a structure of HO···H_wO_w···HO. (The OH and O_wH_w groups are those of the vicinal diol and water, respectively.) This structure is a local energy minimum for the gas-phase monohydrate, and also corresponds to a favorable arrangement in aqueous solution. Klein found, however, BCPs, and concluded that intramolecular hydrogen bonds exist for nonvicinal diols, i.e., when there is at least one $-CH_2-$ group between the substituted carbons of the chain.

In a compilation of our HF/6-31G* O−H stretching frequencies for alcoholic, acidic, and phenolic OH groups,[34] we did not find large deviations from the reference OH frequencies even in conformations where intramolecular O−H···O bonds could be hypothesized. The HF/6-31G* stretching frequencies may be overestimated by about 10%,[8,14] yet trends can reflect the involvement in a H-bond. The calculated largest deviation was smaller than 40 cm^{-1} for 1,2-ethanediol and for some 2-hydroxybenzoic acid conformers. However, the phenolic OH stretching frequency decreased by 160−200 cm^{-1} when the phenolic hydrogen pointed toward the carbonyl oxygen of the −COOH group. For structure 1 in ref 33, the ═O···HO distance is 1.851 Å, which is favorable for a hydrogen bond, although the ═O···H−O angle of 141.1° is still strongly bent in a six-membered ring. Such structures can, however, form intramolecular hydrogen bonds, as was pointed out by Klein on the basis of a BCP for the six-membered rings of 1,3-diols.[36]

Combining the above results and applying them to the analysis of the protonated norepinephrine, we conclude that there is a strained O···H−N intramolecular hydrogen bond in the G1 and T conformations. These conformations are analogues of the tGg′ conformer of a vicinal diol. Table 3 shows that the symmetric and asymmetric N−H vibrations for norepinephrine are in the 3608−3615 and 3703−3745 cm^{-1} ranges, respec-

(32) Alagona, G.; Ghio, C. *Int. J. Quantum Chem.* **2002**, *90*, 641.
(33) (a) Dickinson, J. A.; Hockridge, M. R.; Kroemer, R. T.; Robertson, E. G.; Simons, J. P.; McCombie, J.; Walker, M. *J. Am. Chem. Soc.* **1998**, *120*, 2622. (b) Graham, R. J.; Kroemer, R. T.; Mons, M.; Robertson, E. G.; Snoek, L.; Simons, J. P. *J. Phys. Chem. A* **1999**, *103*, 9706. (c) Butz, P.; Krömer, R. T.; Macleod, N. A.; Simons, J. P. *J. Phys. Chem. A* **2001**, *105*, 544. (d) Unamuno, I.; Fernandez, J. A.; Longarte, A.; Castano, F. *J. Phys. Chem. A* **2001**, *105*, 11524.
(34) Nagy, P. I.; Dunn, W. J., III; Alagona, G.; Ghio, C. *J. Phys. Chem.* **1993**, *97*, 4628.
(35) Bader, R. F. W. *Atoms in Molecules − A Quantum Theory*; Oxford University Press: Oxford, 1990.
(36) Klein, R. A. *J. Comput. Chem.* **2002**, *23*, 585.

Table 2. Optimized Torsion Angles for the Protonated Norepinephrine[a]

	$C_1C_\beta C_\alpha N$	$C_6C_1C_\beta C_\alpha$	$OC_\beta C_\alpha N$	$HOC_\beta C_\alpha$
		G1(1)		
HF/6-31G*	−68.4 (−63.0)[b]	−86.0 (−86.4)	54.4 (60.7)	176.3 (178.5)
MP2/6-31G*	−66.2	−85.3	55.4	−179.2
B3LYP/6-31G*	−68.0	−88.6	54.6	−176.9
MP2/6-311++G**	−64.5	−84.9	57.4	178.0
		G1(2)		
HF/6-31G*	−67.0	−77.4	55.7	168.9
MP2/6-31G*	−64.9	−77.0	56.6	173.7
B3LYP/6-31G*	−66.6	−79.7	55.9	176.0
MP2/6-311++G**	−62.5	−74.5	59.1	170.9
		G1(3)		
HF/6-31G*	−67.7	101.1	54.9	172.0
MP2/6-31G*	−65.6	95.3	55.8	177.5
B3LYP/6-31G*	−67.2	94.1	55.2	−179.7
MP2/6-311++G**	−63.3	97.4	58.3	175.2
		G1(4)		
HF/6-31G*	−67.7	95.7	54.9	175.4
MP2/6-31G*	−65.6	90.6	55.7	−179.4
B3LYP/6-31G*	−67.2	90.3	55.2	−177.0
MP2/6-311++G**	−63.6	91.4	58.0	178.3
		G2(1)		
HF/6-31G*	53.7 (55.3)[b]	−110.1 (−110.0)	176.4 (178.0)	−177.9(−177.1)
MP2/6-31G*	53.4	−101.4	175.1	−177.9
B3LYP/6-31G*	54.6	−100.6	177.4	−177.5
MP2/6-311++G**	45.0	−113.5	167.4	−179.0
		G2(2)		
HF/6-31G*	55.1	−102.5	177.7	176.7
MP2/6-31G*	53.5	−95.6	175.2	176.5
B3LYP/6-31G*	54.2	−95.5	177.0	176.5
MP2/6-311++G**	48.2	−103.4	170.6	176.7
		G2(3)		
HF/6-31G*	55.1 (56.4)[b]	79.2 (79.1)	177.6 (179.0)	178.1 (179.0)
MP2/6-31G*	53.8	79.7	175.5	178.9
B3LYP/6-31G*	53.4	82.7	176.9	179.2
MP2/6-311++G**	47.6	69.7	169.9	179.2
		G2(4)		
HF/6-31G*	51.8	68.4	174.5	−178.1
MP2/6-31G*	47.5	66.5	169.2	−178.3
B3LYP/6-31G*	49.9	69.5	172.5	−177.4
MP2/6-311++G**	44.2	60.6	166.6	−177.8
		T(1)		
HF/6-31G*	−169.7 (−173.1)[b]	−106.3 (−105.0)	−46.7 (−49.7)	−168.3 (−172.8)
MP2/6-31G*	−168.0	−107.0	−46.1	−166.3
B3LYP/6-31G*	−166.9	−108.6	−44.1	−167.4
MP2/6-311++G**	−168.9	−112.3	−46.2	−165.3
		T(2)		
HF/6-31G*	−171.8	−102.0	−48.4	−173.9
MP2/6-31G*	−170.1	−102.0	−47.9	−173.0
B3LYP/6-31G*	−169.2	−105.2	−46.0	−174.2
MP2/6-311++G**	−170.9	−107.0	−47.9	−170.9
		T(3)		
HF/6-31G*	−171.8	80.5	−48.6	−172.3
MP2/6-31G*	−169.7	75.8	−47.7	−170.3
B3LYP/6-31G*	−168.8	75.5	−45.9	−171.1
MP2/6-311++G**	−171.2	69.3	−48.5	−168.0
		T(4)		
HF/6-31G*	−170.1	74.5	−47.1	−168.1
MP2/6-31G*	−168.0	70.7	−46.1	−165.1
B3LYP/6-31G*	−166.9	69.5	−44.1	−165.3
MP2/6-311++G**	−170.4	71.6	−46.9	−167.3

[a] Torsion angles in degrees. Negative values can be converted into the corresponding positive values used in Figures 1−4 by adding 360 to the number. [b] Values in parentheses were obtained for the optimized monohydrate.

tively. The corresponding frequencies for the protonated methylamine, $CH_3NH_3^+$, are 3623 and 3723 cm^{-1} (degenerated) in that table. Shifts are 22 cm^{-1} at most, similar to that for the O−H stretching frequency of 4094 cm^{-1} compared to 4116 cm^{-1} in the free CH_3OH. An intramolecular H-bond was hypothesized for the g3H$^+$ structure of histamine,[2b] where one of the NH_3^+ hydrogens is at a distance of 1.859 Å from the basic nitrogen of the imidazole ring. The N−H stretching frequencies were calculated at 3301, 3687, and 3755 cm^{-1} at the HF/6-31G* level. These values are very close to those for

Table 3. Selected Wavenumbers and Optimized Geometric Parameters at the HF/6-31G* Level for the Protonated Norepineprine and the $CH_3OH\cdots{}^+H_3N-CH_3$ Model Dimer[a]

norepinephrineH^+	G1(1)	G2(1)	G2(3)	T(1)
$C_6C_1C_\beta C_\alpha$ (tors)	55 (47)[b]	37 (52)	49 (59)	52 (40)
$C_1C_\beta C_\alpha$ (bend)	87 (87)[b]	76 (79)	82 (84)	88 (86)
$C_1C_\beta C_\alpha N$ (tors)	138 (139)[b]	130 (143)	131 (138)	109 (114)
$C_\beta C_\alpha NH$ (tors)	269 (302)[b]	227 (319)	239 (330)	245 (264)
N−H (str)				
sym	3615 (3667)[b]	3612 (3667)	3608 (3664)	3613 (3690)
asym	3703 (3415)[b]	3710 (3455)	3705 (3457)	3713 (3416)
	3743 (3744)[b]	3739 (3737)	3737 (3734)	3745 (3755)
O−H (str)	4085	4089	4087	4086
R(N−H···O)	2.232			2.105
A(N−H···O)	102.8			106.7
$CH_3OH\cdots{}^+H_3N-CH_3$				
N−H (str)[e,f]	3329, 3682, 3746 (3623 a_1, 3723 e)		*R*(O−H)[h]	0.946 (0.946)
O−H (str)[g,h]	4094 (4116)		*A*(N−H···O)[d]	174.0
R(N−H···O)[c]	1.756		τ(CONC)[i]	95.1
R(N−H)[f]	1.030, 1.010, 1.010 (1.012)			

[a] Wavenumbers in inverse centimeters. [b] Wavenumbers in parentheses refer to the monohydrate. [c] Shortest N−H···O distance in angstroms. [d] Bond angle (deg) for the hydrogen bond. [e] Wavenumbers in the dimer. [f] Values in parentheses for the isolated $CH_3NH_3^+$. [g] Wavenumber in the dimer. [h] Value in parentheses for the isolated CH_3OH. [i] Torsion angle in deg.

the $CH_3-O(H)\cdots{}^+H_3N-CH_3$ model system (Table 3). The methanol-protonated methylamine dimer is a model of the HO−CH−CH_2−NH_3^+ moiety in protonated norepinephrine. HF/6-31G* geometry optimization could find favorable arrangement for an *intermolecular* hydrogen bond within the dimer. The H-bond parameters are *R*(O···H−N) = 1.755 Å and 174.0° for the O···H−N angle. These parameters characterize a favorable, nearly linear arrangement of the O···H−N moiety. The consequence is a large red shift in one of the N−H stretching frequencies. The optimized geometry for the dimer cannot be reached, however, within protonated norepinephrine because of geometry constraints. The tGg′ analogue structures cannot provide such a short O···H distance with a moderately bent O···H−N arrangement, the lack of which is the main hindrance for a favorable hydrogen bond in the 1,2-substituted ethanes. Hydrogen bond formation or the lack of it can hardly be followed in the shift of the alcoholic O−H frequency. This frequency shows a red shift of only 22 cm^{-1} to 4094 cm^{-1} in the model dimer, whereas the O−H frequencies are 4085−4089 cm^{-1} in norepinephrine. The O−H distance practically does not change in methanol upon dimer formation.

Since our goal is the determination of the equilibrium conformer composition in aqueous solution, monohydrate geometries have also been considered. The difference in the isolated and hydrated protonated norepinephrine geometries reveals the importance of the HO···HNH_2^+ stabilization in the G1 and T conformations as compared to a more relaxed stabilization of the NH_3^+ group connecting to a water oxygen. Values in parentheses in Table 2 show that the key torsion angles, $C_1C_\beta C_\alpha N$ and $OC_\beta C_\alpha N$, change by 3−6° in the G1(1) and T(1) monohydrates. Changes for these torsion angles are smaller, 1−3° for the G2(1) and G2(3) conformers. This latter finding is not surprising because of the nearly trans O···N arrangement without the possibility for an intramolecular hydrogen bond. For G2 conformers, one may expect a relaxed structure even in the gas phase.

For the G1 and T structures, the geometry may allow an intramolecular hydrogen bond. Although it is strongly bent for these conformers, and thus can be considered as a strained hydrogen bond, the structure is still optimal for the isolated molecule. Seemingly small changes in the key torsion angles upon optimization in monohydrates lead to an increase of the internal energy for the G1(1) and T(1) structures themselves by more than 1 kcal/mol. The larger stability of the isolated structure, however, is not reflected in an expected decrease of one of the N−H stretching frequencies.

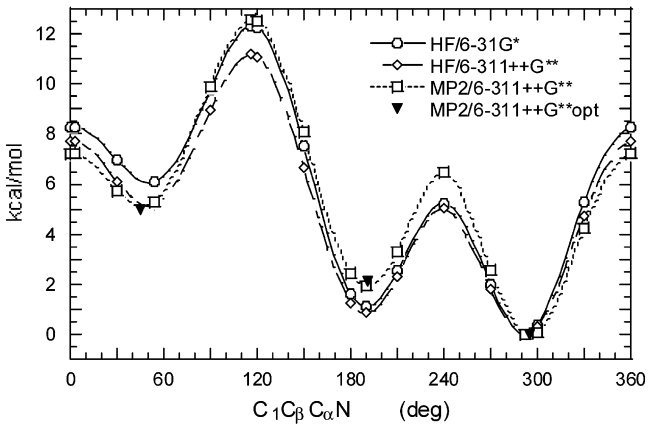

Figure 1. Potential energy profiles for the G2−T−G1 interconversion with HF/6-31G* geometries at various levels (see the legend) with respect to that of G1 taken as zero. The solid triangles refer to the G2, T, and G1 conformers optimized at the MP2/ 6-311++G** level.

This frequency decrease is clearly seen, however, for the monohydrates. The lowest N−H stretching values are in the range of 3415−3457 cm^{-1}, whereas other frequencies are in the range of 3664−3755 cm^{-1}. The trend is the same as with the $CH_3O(H)\cdots{}^+H_3N-CH_3$ dimer (Table 3).

Gas-Phase Energies. In their former paper,[32] Alagona and Ghio published several HF/6-31G* potential energy curves and maps regarding ϑ, φ_2, φ_3, and φ_4 rotations (Chart 2) for protonated norepinephrine. The key rotation characterizing the main conformational differences for the molecule is, however, the φ_1 rotation about the $C_\beta-C_\alpha$ axis. Figure 1 shows the energy as a function of the $\varphi_1 = C_1C_\beta C_\alpha N$ torsion angle up to the MP2/6-311++G**//HF/6-31G* level. MP2/6-311++G**-optimized values for G1(1), T(1), and G2(1) conformers are also indicated.

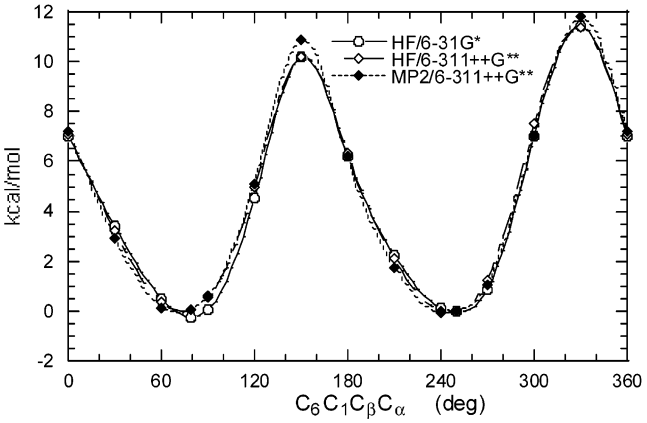

Figure 2. Potential energy profiles for the G2(3)−G2(1) interconversion on the HF/6-31G* geometries at various levels (see the legend) with respect to that of G2(1) taken as zero.

The three rotational curves, with a 3-fold maximum−minimum pattern separated by about 120°, show similar characteristics with some variation in the barrier heights. For the G1 to T barrier at $C_1C_\beta C_\alpha N = 240°$, the HF values with the 6-31G* and 6-311++G** basis sets are 5.25 and 5.02 kcal/mol, respectively. The MP2 value is 6.45 kcal/mol here. The top values at $C_1C_\beta C_\alpha N = 120°$ (T to G2 barrier) are 12.26, 11.09, and 12.49 kcal/mol at the HF/6-31G*, HF/6-311++G**, and MP2/ 6-311++G** levels, respectively. Finally, the G2 to G1 barriers at $C_1C_\beta C_\alpha N = 0°$ or 360° are 8.25, 7.73, and 7.22 kcal/mol at the three levels. All together, considering the indicated levels, the barrier heights can be predicted within a range of 1.5 kcal/mol. Thus, we predict T(1), G(2), and G(1) barriers of 5.0−6.5, 11.1−12.5, and 7.2−8.3 kcal/mol, respectively. The large asymmetry of these rotational potential curves indicates that in cases where two polar groups can approach each other in some conformations but not in others, no simple torsion potentials can be applied for such systems. Thus, molecular mechanics calculations must take care of this special class of 1,2-disubstituted ethane derivatives.

The $\vartheta = C_6C_1C_\beta C_\alpha$ rotational energy curves are compared in Figure 2 for the G2 conformer, whose G2(1) energies are taken as zero. The HF/6-31G*-optimized curve has already been published.[32] In the present study, the variations at the HF/6-311++G**//HF/6-31G* and MP2/6-311++G**//HF/6-31G* levels are shown. The three curves run very close to each other, showing two barriers separated by 180°. The MP2 values are higher by about 0.5 kcal/mol than the other two at the top of the barrier at $\vartheta = 150°$ and 330°. The minima at 79.2° and 249.9° (or, equivalently, −110.1°; see Table 2) correspond to the G2(3) and G2(1) structures, respectively. Thus, the two minima are related by a rotation of 170° for the phenyl ring, leading to the appearance of the 3-OH ring substituent on the opposite face of the receptor site in a bound form. This may have importance in the biological effect of norepinephrine as far as its binding to a receptor is concerned (see the relevant section later on). If the molecule can override the barrier of 10−11 kcal/mol at $\vartheta = 150°$ (which is lower by about 1 kcal/mol than the barrier at $\vartheta = 330°$), then the 3-OH group in its new position can form, for example, a favorable intermolecular hydrogen bond to the receptor. Notice that also the orientation of the 4-OH group is changed.

Utilizing the optimized HF/6-31G* geometries, single-point calculations, up to the QCISD(T) level[11] and using the 6-31G* basis set, were performed for 12 conformers (Table 4). The general conclusion is that relative conformer energies are very close to each other in the MP2, MP3, ..., QCISD(T) series, and are larger by up to 0.9 kcal/mol than the HF/6-31G* values. We found a similar low fluctuation of the relative conformer energies for dopamine[3d] when the theoretical sophistication of the methods was increased. The T conformers are less stable by about 1 kcal/mol further than the G1 rotamers for both protonated dopamine and norepinephrine in the present study when the theory is upgraded from the HF/6-31G* level. In the absence of an OH substitution at C_β in dopamine, G1 and G2 conformers differ only in the rotational position of the phenyl group relative to the NH_3^+ group. The OH substitution, however, differentiates considerably for the G1 and G2 conformers of norepinephrine. For dopamine, the G2−G1 values are 0.3 kcal/mol or less in absolute values. The corresponding values for norepinephrine are in the 6−9 kcal/mol range. Thus, the β-OH substitution in this molecule does not simply mean a change in the chemical structure, but also leads to a marked stabilization of the G1 conformers as compared to the G2 ones in the gas phase.

Relative conformer energies calculated after geometry optimization up to the MP2/6-311++G** level are compared in Table 5. Although there are some changes as compared to the values in Table 4, and new calculations at the B3LYP/6-31G* level are also included, the basic conclusions remain unaltered. The G1 conformers, specifically G1(1) and G1(3), are the most stable ones in the gas phase. The T(1) and T(3) conformers are higher in energy than G(1) by 1.1−1.5 kcal/mol at both the

Table 4. Relative Energies at Different Levels Calculated at the HF/6-31G*-Optimized Geometries and with the 6-31G* Basis Set for the Protonated Norepinephrine in the Gas Phase[a]

	HF	MP2	MP3	MP4SDQ	QCISD	QCISD(T)
G1(1)	0.00	0.00	0.00	0.00	0.00	0.00
G1(2)	2.50	2.76	2.68	2.70	2.70	2.70
G1(3)	0.33	0.57	0.47	0.45	0.48	0.53
G1(4)	1.63	1.63	1.66	1.62	1.66	1.66
G2(1)	6.09	6.81	6.78	6.75	6.80	6.82
G2(2)	6.93	7.43	7.46	7.44	7.49	7.47
G2(3)	5.84	6.39	6.35	6.38	6.39	6.38
G2(4)	8.01	8.82	8.78	8.80	8.82	8.80
T(1)	1.10	2.01	1.78	1.80	1.79	1.89
T(2)	2.87	3.76	3.58	3.56	3.55	3.64
T(3)	1.46	2.39	2.16	2.19	2.17	2.27
T(4)	2.96	3.72	3.59	3.60	3.59	3.64

[a] Energies in kilocalories per mole.

Table 5. Relative Energies at Optimized Geometries for the Protonated Norepinephrine in the Gas Phase[a]

	HF/6-31G*	MP2/6-31G*	B3LYP/6-31G*	HF/6-311++G**	MP2/6-311++G**
G1(1)	0.00	0.00	0.00	0.00	0.00
G1(2)	2.50	2.60	2.64	2.39	2.23
G1(3)	0.33	0.51	0.44	0.24	0.38
G1(4)	1.63	1.54	1.39	1.65	1.45
G2(1)	6.08	6.72	5.91	5.12	4.96
G2(2)	6.93	7.24	6.43	6.21	5.87
G2(3)	5.84	6.31	5.61	5.17	5.07
G2(4)	8.01	8.64	7.86	7.14	6.60
T(1)	1.10	2.27	1.08	0.86	2.11
T(2)	2.87	4.00	2.69	2.68	3.78
T(3)	1.46	2.66	1.46	1.26	2.56
T(4)	2.96	3.97	2.62	2.78	3.74

[a] Energies in kilocalories per mole.

Table 6. Free Energy Correction Terms Relative to the G1(1) Conformer in the Gas Phase at $T = 310$ K and $p = 1$ atm[a]

	ΔZPE		$\Delta(H_{vibr}(T) - ZPE)$		$-T\Delta S_{vibr}(T)$		$-T\Delta S_{tot}(T)$		$\Delta G_{th}(T)$	
	usc[b]	sc[c]	usc	sc	usc	sc	usc	sc	usc	sc
G2(1)	−0.41	−0.38	0.20	0.18	−0.70	−0.68	−0.72	−0.70	−0.93	−0.90
G2(3)	−0.35	−0.32	0.15	0.14	−0.41	−0.39	−0.43	−0.42	−0.63	−0.60
T(1)	−0.23	−0.21	0.12	0.11	−0.33	−0.32	−0.37	−0.36	−0.48	−0.46
TS1[d]	−0.21	−0.23	−0.41	−0.41	0.87	0.87	0.87	0.88	0.25	0.24
TS2[d]	−0.43	−0.41	−0.34	−0.34	0.58	0.58	0.51	0.52	−0.26	−0.24
TS3[d]	−0.14	−0.15	−0.35	−0.35	0.55	0.55	0.51	0.52	0.02	0.01
TS4[e]	−0.61	−0.56	−0.30	−0.32	0.96	0.98	0.91	0.93	0.00	0.05
TS5[e]	−0.67	−0.62	−0.29	−0.31	0.87	0.89	0.82	0.84	−0.14	−0.09

[a] Correction terms in kilocalories per mole. [b] Unscaled frequencies. [c] Scaled frequencies; for details, see the text. [d] Transition states throughout rotations about the $C_\beta-C_\alpha$ axis. $C_1C_\beta C_\alpha N$ torsion angles for the TS1, TS2, and TS3 structures are 2.9°, 116.4°, and 239.8°, respectively. [e] Transition states throughout rotations about the C_1-C_β axis. $C_6C_1C_\beta C_\alpha$ torsion angles for the TS4 and TS5 structures are 149.1° and 322.6°, respectively.

HF/6-31G* and B3LYP/6-31G* levels, and by 2.1−2.7 kcal/mol at the MP2 level, when geometry optimization is performed with either the 6-31G* or 6-311++G** basis set. G2(1) and G2(3) relative energies are similar, 5.6−6.1 kcal/mol at the HF/6-31G* and B3LYP/6-31G* levels, but G2(1) and G2(3) are both remarkably stabilized by 1.1 and 0.8 kcal/mol, respectively, upon MP2/6-311++G** optimization. HF/6-311++G** geometry optimizations lead to small, 0.1−0.2 kcal/mol, stabilization of the G1 (with the exception of G1(4)) and T conformers as compared to the HF/6-31G* results. The effect of the basis set extension is larger (0.7−1.0 kcal/mol) for the G2 conformers.

On the basis of the data in Table 5, it is difficult to assess the combined effect of the basis set extension and consideration of the electron correlation. MP2/6-31G* values are always remarkably larger than HF/6-31G* values for the G2 and T conformers. More surprisingly, the values from B3LYP calculations, where electron correlation is included in the functional, are close to the HF data, and are smaller (with one exception) than the corresponding MP2 values. A possible reason for the difference between the B3LYP and MP2 values is that MP2 includes dispersion contributions, too, not considered by the DFT/B3LYP description. With the 6-311++G** basis set, the trend is not obvious. Relative HF and MP2 values are almost equal for G1(2), and MP2 values are slightly smaller than HF values for G2, and are larger by more than 1 kcal/mol for the T conformers. For dopamine, we found a 1 kcal/mol increase of the T conformer energy when comparing B3LYP to HF values with separate geometry optimizations with the 6-31G* basis set. Optimization at the MP2/6-311++G** level for dopamine[3d] resulted in a 2.3 kcal/mol increase of the relative energy for T as compared to the HF/6-31G* value. This increase is only about 1 kcal/mol in Table 5 for norepinephrine.

The equilibrium conformer composition is, however, a function of the free energy difference, not of the internal energy. The composition is a sensitive function of $\Delta G°$. For example, $\Delta G° = 0.85$ kcal/mol corresponds to a conformer ratio of 1:4 at $T = 310$ K. Some $\Delta G_{th}(T)$ thermal correction values in Table 6 are close to this free energy difference; thus, it is important to analyze the calculated values.

The immediate impression from this table is that the scaling procedure has negligible effect on the *relative* ZPE and thermal correction terms for local-energy-minimum conformers G2(1), G2(3), and T(1). (Values in the table are provided relative to the corresponding G1(1) values.) Values without scaling (usc) and after it (sc) differ by no more than 0.03 kcal/mol. Some of the values themselves are, however, remarkable. The $-T\Delta S_{tot}(T)$ entropy term dominates $\Delta G_{th}(T)$, whereas opposite signs for ΔZPE and $\Delta(H_{vibr}(T) - ZPE)$ (accounting for the thermal excitation enthalpy of the vibrations) lead to partial cancellation of those terms.

The largest contribution to the total relative entropy comes from the vibrational part, $T\Delta S_{vibr}(T)$. Since the translational entropy is constant for conformers, $T\Delta S_{tot}(T) - T\Delta S_{vibr}(T) = T\Delta S_{rot}(T)$. The latter values are 0.02−0.04 kcal/mol; thus, the relative rotational entropies are really small (up to 40/310 cal/(deg mol)). This means that the change of the moments of inertia, determining $\Delta S_{rot}(T)$, is small for the protonated norepinephrine conformers, or at least the product of the moments remains nearly constant.[12]

$T\Delta S_{vibr}(T)$ is conspicuously large for G2(1). A closer investigation shows that the lowest vibration with a frequency of 37 cm^{-1} (as compared to 55 cm^{-1} for G1(1), Table 3) has a $-T\Delta S_{vibr1}(T)$ contribution of −0.23 kcal/mol. The relatively large value is a consequence of this low frequency. This vibration corresponds to the $C_6C_1C_\beta C_\alpha$ torsion. The third lowest frequency motion refers to the $C_1C_\beta C_\alpha N$ torsion. One may raise the question of whether these torsions are really vibrations or whether they could be better characterized as hindered rotations. Figure 2 indicates a barrier of at least 10 kcal/mol to the rotation for the phenyl group. This large value seems to be prohibitive for even a hindered rotation. We consider the barrier of at least 4 kcal/mol (T(1) to G1(1), Figure 1) as preventing the rotation of the whole NH_3^+ group about the $C_\beta-C_\alpha$ axis *in the gas phase*. The barriers can, however, be reduced upon solvation, and this problem will be studied in the next section.

The $C_\beta C_\alpha NH$ torsional vibrations take place with wavenumbers of 227−269 cm^{-1}. For G2(3), the ground state is $0.002859(239/2) = 0.34$ kcal/mol above the potential minimum. The potential curve for the $-NH_3^+$ rotation about the $C_\alpha-N$ bond shows a barrier of 2.49 kcal/mol for G2(3). Thus, the vibrational excitation energy must be $2.49 - 0.34 = 2.15$ kcal/mol for overriding the barrier. At $T = 310$ K it means that less than 3% of the molecules possess this activation energy, as calculated from the Boltzmann distribution.

The values in parentheses in Table 3 refer to the corresponding frequencies assigned in the monohydrates. They show the increase of the $C_6C_1C_\beta C_\alpha$ torsion frequency for the G2 conformers, and the decrease of these values for G1 and T. Even 10−15 cm^{-1} changes in these values are important, because very low values give the largest contribution to the vibrational entropy. Indeed, the scaled $-T\Delta S_{vibr}(T)$ values for the gas-phase G2(1) and G2(3) conformers change from −0.68 and −0.39 kcal/mol (Table 6) to −0.31 and −0.18 kcal/mol, respectively, in the monohydrates. The total scaled $\Delta G_{th}(T)$ values for G2(1),

Table 7. Relative Free Energies in Solution: United-Atom Force Field[a]

	$C_1C_\beta C_\alpha N$	ΔE		ΔG_{th}		$\Delta G°$(solv)		$\Delta G°$(tot)	
	g	g	mh	g	mh	g	mh	g	mh
TS1	2.9	8.27		0.24		−3.64		4.87	
G2(1)	53.7	6.08	6.28	−0.90	−0.56	−6.44	−6.64	−1.26	−0.92
TS2	116.4	12.32		−0.24		−8.50		3.58	
T(1)	190.3	1.10	2.40	−0.46	−0.62	−0.71	−2.55	−0.07	−0.77
TS3	239.8	5.25		0.01		−0.08		5.18	
G1(1)	291.7	0.00	1.06	0.00	−0.06	0.00	−1.20	0.00	−0.20
	$C_6C_1C_\beta C_\alpha$	ΔE		ΔG_{th}		$\Delta G°$(solv)		$\Delta G°$(tot)	
	g	g	mh	g	mh	g	mh	g	mh
G2(3)	79.2	5.84	6.03	−0.60	−0.41	−7.10	−7.56	−1.86	−1.94
TS4	149.1	16.27		0.05		−8.68		7.64	
G2(1)	249.9	6.08	6.28	−0.90	−0.56	−6.44	−6.64	−1.26	−0.92
TS5	322.6	17.86		−0.09		−7.75		10.02	

[a] Energy terms in kilocalories per mole, torsion angles in degrees. Codes g and mh refer to the geometry optimized in the gas phase and in the monohydrate, respectively, at the HF/6-31G* level. ΔE values were calculated at the HF/6-31G* level. All terms ΔE, ΔG_{th}, and $\Delta G°$(solv) are given relative to those of the gas-phase G1(1) conformer with $C_1C_\beta C_\alpha N = 291.7°$ and $C_6C_1C_\beta C_\alpha = 0°$.

G2(3), and T(1) are −0.51, −0.36, and −0.57 kcal/mol, with reference to those of the monohydrate G1(1) structure. (Values relative to those for the isolated G1(1) structure, which is the general reference point in this paper, are given in Table 7.) Thus, upon monohydration the thermal corrections change by up to 0.4 kcal/mol, as compared to the values in Table 6.

The $-NH_3^+$ hindered rotation for G2(3) becomes more feasible in the monohydrate than in the gas phase, but the $C_\beta C_\alpha$-NH torsional motion can still be characterized primarily as a vibration. The harmonic frequency is 330 cm^{-1}; thus, the ground state is above the potential minimum by 0.47 kcal/mol. The potential curve is asymmetric for the torsional motion with barriers of 2.43 and 2.77 kcal/mol for the back and forth rotations. Less than 4% of the molecules have the necessary activation energy for overriding the lower barrier.

The barrier to the $-NH_3^+$ rotation for the gas-phase G1(1) conformer is 3.96 kcal/mol. Different G1(1) monohydrates have been identified, and a barrier height of at least 2.29 kcal/mol was found. The ground state in this case is above the minimum by 0.43 kcal/mol (302/2 cm^{-1}), and less than 5% of the molecules possess the necessary thermal activation energy allowing a turnover for the $-NH_3^+$ group. Thus, the chances for a hindered rotation in aqueous solution are similar for the G2(3) and G1(1) conformers, and the difference in the thermal free energy correction should nearly be constant with either an only-vibration or a combined vibration-hindered rotation model.

Free energy corrections have also been calculated for the transition states throughout the rotations shown in Figures 1 and 2. The values have been calculated by neglecting the imaginary frequencies. The effect of scaling is small here as well, amounting to a 0.05 kcal/mol difference in the two procedures. As a result of the more effective term cancellation here than for local-minimum-energy structures, the relative ΔG_{th}-(T) terms are considerably smaller than those for local minima, and influence the free energy of the barrier by less than 0.3 kcal/mol.

Equilibrium in Solution. Using the united-atom model, the change in the solvation free energy throughout the rotations about the $C_\beta-C_\alpha$ and C_1-C_β axes are depicted in Figures 3 and 4, respectively. Rotation of the NH_3^+ group, as a whole, about the $C_\beta-C_\alpha$ axis entails large changes in the solvation free energy. Starting from the CCCN eclipsed conformation, i.e., with $C_1C_\beta C_\alpha N = \varphi_1 = 0°$, $G°$(solv) decreases by about 6 kcal/mol and reaches its minimum value at about $\varphi_1 = 100°$. (The value at $\varphi_1 = 0°$ is −3.48 kcal/mol, because the reference conformation is G1(1) with $\varphi_1 = 291.7°$.) $G°$(solv) steeply increases between $\varphi_1 = 100°$ and $\varphi_1 = 210°$, stays almost constant until 291.7° (G1(1)), and decreases by 3.5 kcal/mol when $\varphi_1 = 360° = 0°$ is reached. As mentioned before, the total change throughout the entire 360° rotation is 0.14 ± 0.31 kcal/mol.

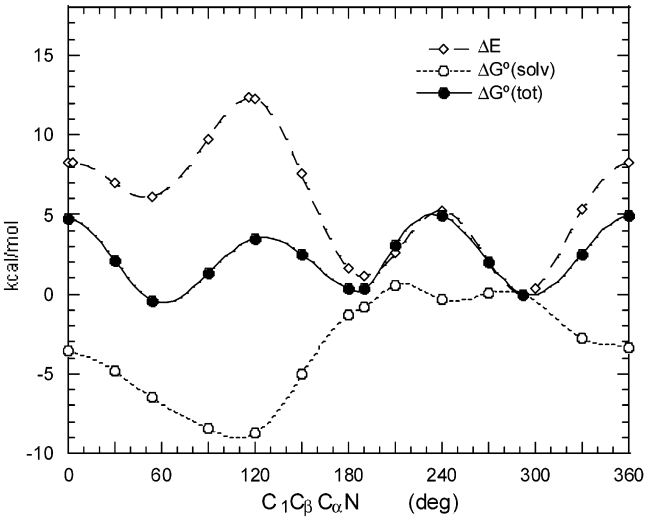

Figure 3. Free energy profile in solution, $\Delta G°$(tot), and its components, ΔE, the HF-6-31G* internal energy, and $\Delta G°$(solv), computed from the MC free energy perturbation simulations, using the united-atom force field, for the G2−T−G1 interconversion (see the legend) with respect to those for G1 taken as zero. Thermal corrections are not included in $\Delta G°$(tot).

The consequence of the large solvent effect in the 0−210° torsion range is seen in Figure 3. The sum of the HF/6-31G* ΔE and $\Delta G°$(solv) curves provides a 3-fold rotation potential with a much more balanced minimum−maximum pattern than was the case for the gas-phase curve. Table 7 reports free energy data for the G1(1), T(1), and G2(1) minima and the TS1, TS2, and TS3 maxima (gas-phase transition states). From these data, the TS1−G2−TS2−T−TS3−G1−TS1 free energy separations in solution are −6.13, 4.84, −3.65, 5.25, −5.18, and 4.87 kcal/mol, respectively. The corresponding gas-phase values are −3.33, 6.90, −11.44, 4.62, −5.26, and 8.51 kcal/mol. Thus, the

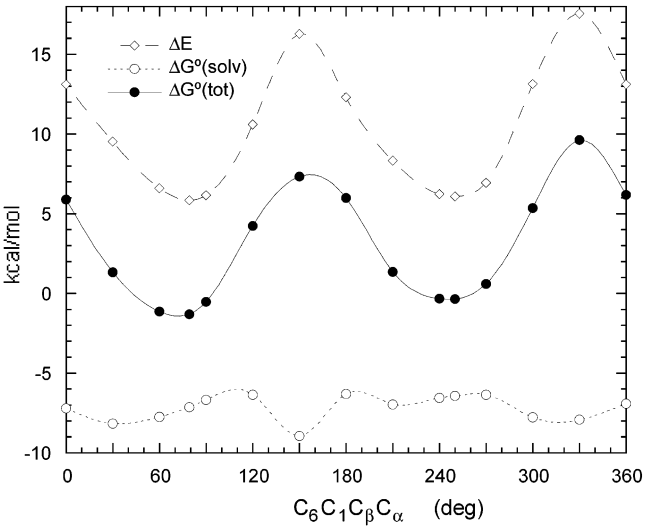

Figure 4. Free energy profile in solution, $\Delta G°$(tot), and its components, ΔE, the HF-6-31G* internal energy, and $\Delta G°$(solv), computed from the MC free energy perturbation simulations, using the united-atom force field, for the G2(3)−G2(1) interconversion (see the legend) with respect to those for G1 taken as zero. Thermal corrections are not included in $\Delta G°$(tot).

interaction with the water solvent leads to a "smoothing" effect on the torsion potential curve: large barriers decrease (from 11.44 to 3.65 kcal/mol for T → TS2, from 8.51 to 4.87 kcal/mol for G1 → TS1) and small barriers increase (3.33 to 6.13 for G2 → TS1) upon $C_1C_\beta C_\alpha N$ rotation. There is almost no solvent effect on the medium-height G1 to TS3 barrier. All these analyses are based on the HF/6-31G* relative energies, but should be primarily valid at other levels of ab initio calculations, given the similarity of the gas-phase curves in Figure 1.

A similar analysis can be carried out for the $C_6C_1C_\beta C_\alpha$ rotation (Figure 4). The gas-phase curve describes a 2-fold torsion potential with two slightly different barriers. In contrast, however, to the $C_1C_\beta C_\alpha N$ curve, the solvent effect is small for the phenyl rotation. Starting from the $\vartheta(C_6C_1C_\beta C_\alpha) = 0°$ reference state, the solvation free energy change is no more than 1.72 kcal/mol, with the minimum value at $\vartheta = 150°$. Changes of the in-solution free energies for the G2(3)−TS4−G2(1)−TS5−G2(3) transformations are 9.50, −8.90, 11.28, and −11.88 kcal/mol, respectively. The corresponding gas-phase values are 11.08, −11.14, 12.59, and −12.53 kcal/mol. Free energies of the barriers are reduced from 11.08 to 9.50 kcal/mol and from 12.59 to 11.28 kcal/mol upon solvation; thus, in this case both barriers are lowered. The decrease is, however, relatively small, and the 9−12 kcal/mol barriers should prevent the phenyl rotation in aqueous solution. The 3.6−6.1 kcal/mol free energy barriers are considerably smaller for the $C_1C_\beta C_\alpha N$ rotation, but in our opinion, they are still large enough for maintaining well-defined local minimum-free-energy structures, and a measurable conformational equilibrium for the protonated norepinephrine in aqueous solution.

Indeed, Solmajer et al.[37] measured this conformational equilibrium in aqueous solution at variable pH, using high-resolution PMR spectroscopy. Our computer modeling fits best to the experimental conditions at pH 7, where these authors found the T, G1, and G2 conformers in a ratio of 65:24:11. From the data in Table 7 with the gas-phase-optimized conformer geometries, G2(1) is stabilized by 1.19 kcal/mol relative to T(1) and G2(3) is stabilized by 0.60 kcal/mol relative to G2(1) upon phenyl rotation. The free energy difference of 1.79 kcal/mol between G2(3) and T gives a large G2 preference in contrast to the experimental value.

(37) Solmajer, P.; Kocjan, D.; Solmajer, T. *Z. Naturforsch.* **1983**, *38 c*, 758.

Table 8. Relative Free Energies in Solution: All-Atom Force Field[a]

	ΔE	ΔG_{th}	$\Delta G°$(solv)	$\Delta G°$(tot)[b]
		HF/6-31G*		
G1(1)	0.00	0.00	0.00	0.00
T(1)	1.34	−0.56	−2.13 ± 0.24	−1.35
G2(1)	5.22	−0.50	−4.36 ± 0.30	0.36
G2(3)	4.97	−0.35	−5.11 ± 0.56	−0.49
		MP2/6-31G*		
G1(1)	0.00	0.00	0.00	0.00
T(1)	2.50	−0.56	−2.13 ± 0.24	−0.19
G2(1)	5.89	−0.50	−4.36 ± 0.30	1.03
G2(3)	5.49	−0.35	−5.11 ± 0.56	0.03

[a] Energies in kilocalories per mole, HF/6-31G*-optimized monohydrate geometries. [b] The standard deviation for $\Delta G°$(tot) is the same as for $\Delta G°$(solv).

When geometries from optimized monohydrates are used, the overall results change only a little. These calculations reveal, however, that G1(1) and T(1) conformers with these geometries are solvated more preferably by 1.2−1.8 kcal/mol than with their gas-phase structure. The internal energy in the optimized monohydrate is necessarily higher than for the optimized isolated one. The energy increases of 1.1−1.3 kcal/mol for G1(1) and T(1) mainly cancel the gain by solvation. The solvation free energy is also preferable for the G2 conformers by 0.2−0.5 kcal/mol, and the increase of the relative internal energy is about 0.2 kcal/mol for them. Changes in the thermal correction are 0.2−0.3 kcal/mol. Combinations of the terms lead to an overall decrease of the total relative free energy (relative to that of the gas-phase structure G1(1) conformer) by 0.2, 0.7, and 0.1 kcal/mol for G1(1), T(1), and G2(3), respectively, whereas G2(1) is less favorable for the monohydrate geometry by 0.3 kcal/mol. Thus, even with the geometry optimized in the monohydrate, the prevailing conformer is G2(3) when the OPLS-UA force field is used.

The results change dramatically when the OPLS-AA force field is introduced. Table 8 shows that already at the (quantum chemically less reliable) HF/6-31G* level, T(1) is the prevailing conformer and G2 is the second most populated. Table 4 shows that any methods higher than the HF level give nearly equal relative conformational energies, but these values are generally consistently higher than the HF/6-31G* values. Thus, MP2/6-31G* results are comparable with QCISD(T) results with the 6-31G* basis set for norepinephrine. Applying the MP2/6-31G*//HF/6-31G* relative internal energies for the monohydrate-optimized structures, the population is T(1):G1(1):G2(3):G2(1) = 38.9:28.6:27.2:5.4 at 310 K and pH 7 in aqueous solution. Because of the long simulations, only these four conformations have been considered. It is worth mentioning, however, that a more proper composition contains T(3) and G1(3) as well. Taking into account T(3) and G1(3) in the equilibrium mixture will necessarily reduce the G2 fraction and will increase the T and G1 fractions; thus, the theoretical estimate will shift toward the experimental composition. Furthermore, the present study of the equilibrium composition accounts only for the protonated form of norepinephrine at pH

7. At this pH, however, there are 7% mainly neutral and zwitterionic forms in the solution. Their contributions were necessarily included in the experimental composition, but not in the theoretical one.

Alagona and Ghio,[32] using the PCM continuum solvent approach at the HF/6-31G* level and considering three conformers, qualitatively reproduced the experimental composition. In that study the differential stabilizations of the T(1) and G2-(3) conformers were about 2 and 3 kcal/mol relative to G1(1). Albeit the value for T(1) is practically the same, MC/FEP calculations predict a 4−5 kcal/mol more negative solvation free energy for G2 conformers.

Regarding the reliability of the experimental results, one important point has to be mentioned. In the Solmajer experiment "a trace of Na_2SO_3 was added to prevent oxidative destruction of catechol ring hydroxyls".[37] Higuchi and Schroeter found that HSO_3^- anions can replace the alcoholic OH group in norepinephrine at pH 5 or higher.[38] If this reaction took place throughout the experiment, then a norepinephrine sulfonyl derivative was also present in the solution. If all the "trace of Na_2SO_3" reacted, then the system was not protected against oxidation any more, and formation of a *o*-quinonoid structure at the catechol part was also possible. Overall, the reaction conditions were not specified to rule out the presence of several norepinephrine derivatives. Since the conformational equilibrium is sensitive for this molecule, the presence of other compounds in the system could influence the PMR spectra and the derived composition.

Norepinephrine Conformation in a Receptor Cavity. Although modeling of the binding to a receptor cannot be carried out at such a high level as those in the previous calculations, due to its practical importance, an approximate analysis has been performed to obtain the likely conformation of norepinephrine in a receptor cavity. On the basis of research by Strader et al.,[39] a pharmacophore model had been developed for the biogenic amine binding site within the β-adrenergic receptor (βAR). This receptor belongs to the G-protein-coupled receptor superfamily with seven transmembrane (TM) α-helices. The binding model hypothesizes five connections with the ligand: an ion-pair interaction with Asp113 (TM3), a hydrogen bond with the alcoholic OH (Ser165, TM4), hydrogen bonds between the catechol 3-OH and 4-OH groups and the Ser204 and Ser207 (TM5) OH groups, respectively, and a stacking interaction of the aromatic ring with the side chain of Phe290 (TM6). Strader and co-workers also suggested that rhodopsin can serve as a good template for a βAR model.

Thus, we modeled the βAR amine-binding site by utilizing the recent experimental structure for rhodopsin.[40] The side chains for the above five amino acids and their left and right neighbors were modified according to the primary structure of βAR.[39b] The Sybyl 6.6 software was used[41] for these manipulations and the subsequent ligand docking. Norepinephrine was placed in the binding cavity, and a series of manual adjustments followed by a short docking were applied for finding the preferred binding orientation. All-atom AMBER charges[42] were used for the receptor, and charges were retained for norepinephrine from in-solution simulations. Docking was performed using the Tripos force field of Sybyl 6.6, the nonbonded cutoff was set to 8 Å, and the distance-dependent dielectric constant was set to 4.

The favorable conformation of the docked ligand is close to the T(3) structure (see STR3 in Chart 2, and Table 2). There is a strong ionic interaction between the Asp113 carboxylate and the protonated head of the ligand, as indicated by 2.1−2.5 Å long hydrogen bonds between the $-COO^{-}\cdots{}^{+}H_3N-$ groups. The 3-OH and 4-OH groups are hydrogen-bond donors to Ser204 and Ser207, respectively, with H···O separations of 3−4 Å. The aromatic ring is stacked with Phe290 (C···C distances of 4−5.5 Å between the ring atoms). The alcoholic oxygen of norepinephrine was found more than 6 Å from the Ser165 OH; therefore, this hydrogen bond was not possible in the docked orientation. Instead, we found that both the Ser OH and the norepinephrine OH are within about 3−4 Å of the backbone carbonyl of Val 114; thus, the alcoholic OH of the ligand may be the proton donor in an O−H···O=C hydrogen bond.

The docked conformer with $C_1C_\beta C_\alpha N$ and $C_6C_1C_\beta C_\alpha$ torsion angles of −145° and 107°, respectively, meets four out of five of Strader's criteria. It should also be considered that we have not used the full βAR primary structure, and perhaps more important, the experimental *inactive rhodopsin* structure is not a very good template for the binding cavity of βAR. Indeed, Borhan[43] has noted that TM3, TM4, and TM5 undergo a remarkable spatial displacement throughout the activation of rhodopsin. In addition, in a recent study,[44a] TM5 was found too far from TM3 and TM6 in the binding cavity of the muscarinic-1 receptor built up by using rhodopsin as a template, thus implying a minor role for TM5 in the acetylcholine binding, in contrast to some experimental results.[44b] With the present geometry of the helical structure, hydrogen bonds are feasible to Val114, Ser204, and Ser207 only when the ligand leaves the docked, local-minimum-energy position, and performs some roaming motion within the cavity.

The docking studies were performed in the absence of water solvent. The results indicate that the binding cavity is mostly filled in by the norepinephrine ligand, and solvation of the dimer leads to the appearance of only 3−4 water molecules close to the binding site. These water molecules must be, however, very important. If the ligand penetrates into the binding cavity from the extracellular solution, where it takes a protonated form, some water must accompany the ligand along its more than 10 Å long route into the depth of the receptor. Without close water molecules, the maintenance of the protonated state is questionable. Without water at the ion-pair interaction site, it is also questionable whether the proton stays on the amino group or jumps over to the Asp113 carboxylate. For zwitterions, even one nearby water molecule is enough for maintaining the ionic

(38) Higuchi, T.; Schroeter, L. C. *J. Am. Chem. Soc.* **1960**, *82*, 1904.
(39) (a) Tota, M. R.; Candelore, M. R.; Dixon, R. A. F.; Strader, C. D. *Trends Pharmacol. Sci.* **1991**, *12*, 4. (b) Strader, C. D.; Fong, T. M.; Tota, M. R.; Underwood, D. *Annu. Rev. Biochem. Soc.* **1994**, *63*, 101. (c) Cascieri, M. A.; Fong, T. M.; Strader, C. D. *J. Pharmacol. Toxicol. Methods* **1995**, *33*, 179.
(40) Palczewski, K.; Kumasaka, T.; Hori, T.; Behnke, C. A.; Motoshima, H.; Fox, B. A.; Le Trong, I.; Teller, D. C.; Okada, T.; Stenkamp, R. E.; Yamamoto, M.; Miyano, M. *Science* **2000**, *289*, 739.
(41) *Sybyl*, version 6.6; Tripos, Inc.: St. Louis, MO, 1999.
(42) Weiner, S. J.; Kollman, P. A.; Nguyen, D. T.; Case, D. A. *J. Comput. Chem.* **1986**, *7*, 230.
(43) Borhan, B.; Souto, M. L.; Imai, H.; Shichida, Y.; Nakanishi, K. *Science* **2000**, *288*, 2209.
(44) (a) Rajeswaran, W. G.; Cao, Y.; Huang, X.-H.; Wroblewski, M. E.; Colclough, T.; Lee, S.; Liu, F.; Nagy, P. I.; Ellis, J.; Levine, B. A.; Nocka, K. H.; Messer, W. S., Jr. *J. Med. Chem.* **2001**, *44*, 4563 and references therein. (b) Lu, Z.-L.; Saldanha, J. W.; Hulme, E. C. *Trends Pharmacol. Sci.* **2002**, *23*, 140 and references therein.

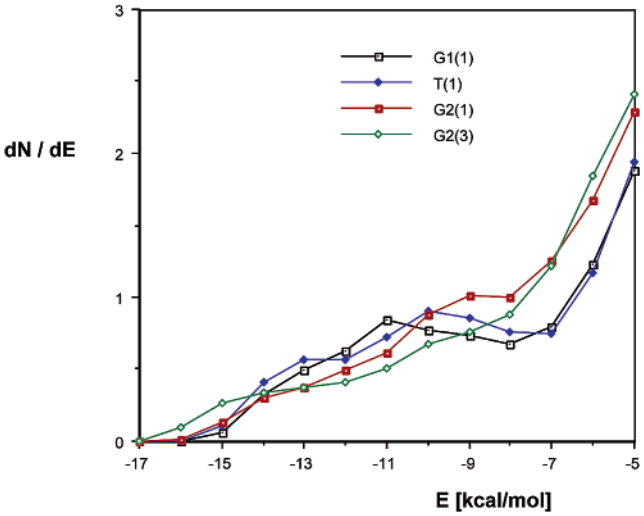

Figure 5. Solute−solvent pair-energy distribution functions (all-atom force field).

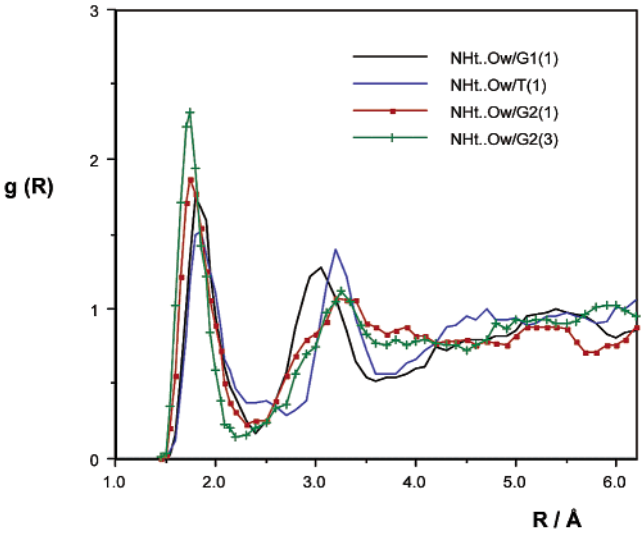

Figure 6. (N)H(trans)···O_w radial distribution functions, all-atom force field.

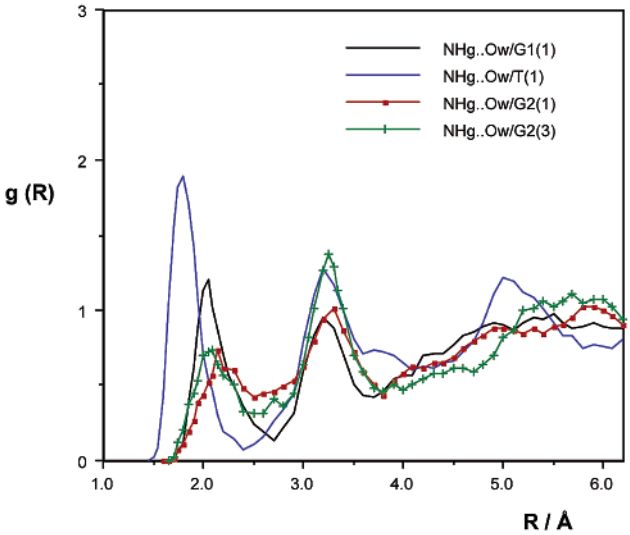

Figure 7. (N)H(gauche)···O_w radial distribution functions, all-atom force field. The gauche hydrogen closer to the phenyl ring has been selected.

interaction.[45a] One or two water molecules are generally sufficient for maintaining stable $A^-\cdots H^+B$ ion pairs or zwitterions.[4b,45b,c] Liljefors and Norrby[46] pointed out that the trimethylammonium−formate ion pair is stable in an environment characterized by a dielectric constant $\epsilon > 9$, or the monohydrate exists in the ion-pair form with $\epsilon > 4-6$. All these results suggest that norepinephrine, in its nearly T(3) conformation, can form an ionic interaction with the Asp113 carboxylate in the βAR binding cavity, However, only very complicated and high-level calculations, including the proper receptor model, can shed some light onto the thermodynamic changes following the penetration of the T(1) or G2(3) conformer of protonated norepinephrine into the binding pocket, and taking its favorable conformation in an environment with only a small number of water molecules.

Solution Structure. The solution structure has been characterized for results obtained with the OPLS-AA force field. Solute−solvent pair-energy distribution functions (pedf's; Figure 5) give the number of water molecules within the interaction-energy range of E and $E + dE$ to the solute. In general, the pedf shows a maximum−minimum shape or at least a shoulder in the negative interaction energy range for polar molecules in aqueous solution. Integration until the minimum (end of the shoulder) gives the number of water molecules in some special interaction with the solute. Many examples[2b,3d,7,21a,b,22] show that this number can reasonably be associated with the number of hydrogen bonds (N_{HB}) between the solute and the water solvent.

For a G2 conformer, the maximum number of strong intermolecular hydrogen bonds is expected. The strongest three are formed to the water-exposed NH_3^+ group. Another is expected to be formed with the alcoholic OH, where the hydrogen was always found in the trans position within the $H-O-C_\beta-C_\alpha$ moiety. The fifth strong hydrogen bond should be formed to the 4-OH ring substituent, also exposed to interaction with water molecules. The 3-OH hydrogen points toward the oxygen of the 4-OH group; henceforth, it is partially shielded from interaction with the solvent. OH groups are stronger hydrogen-bond donors than acceptors;[16,34] thus, hydrogen bonds of the $O_w-H_w\cdots O$(solute) type would have less negative interaction energies, and are expected to contribute to pedf's in their unresolved courses with $E > -7$ kcal/mol.

By integration of the pedf's until $E = -8$ kcal/mol, the following N_{HB} values were obtained: G1(1), 4.5; T(1), 4.9; G2-(1), 4.8; G2(3), 4.3. That for T(1) is 5.7 until $E = -7$ kcal/mol. These values indicate that T(1) rather than a G2 conformer makes the largest number of hydrogen bonds. However, the values do not reflect that G2 conformers form the strongest hydrogen bonds. This can be concluded by noticing that the pedf's for G2 conformers run above those for G1 and T in the range of $E = -17$ to -15 kcal/mol.

The relatively large N_{HB} for T(1) suggests that none of the NH_3^+ hydrogens are shielded from hydration. Thus, even if one N−H points toward the alcoholic oxygen, the N−H···O bond is so bent that the protonated amine can satisfactorily be hydrated. Indeed, all three (N)H···O_w coordination numbers, calculated by integration of the radial distribution functions

(45) (a) Ding, Y.; Krogh-Jesperson, K. *J. Comput. Chem.* **1996**, *17*, 338. (b) Larson, L. J.; Largent, A.; Tao, F.-M. *J. Phys. Chem. A* **1999**, *103*, 6786. (c) Snyder, J. A.; Cazar, A. R.; Jamka, A. J.; Tao, F.-M. *J. Phys. Chem. A* **1999**, *103*, 7719.
(46) Liljefors, T.; Norrby, P.-O. *J. Am. Chem. Soc.* **1997**, *119*, 1052.

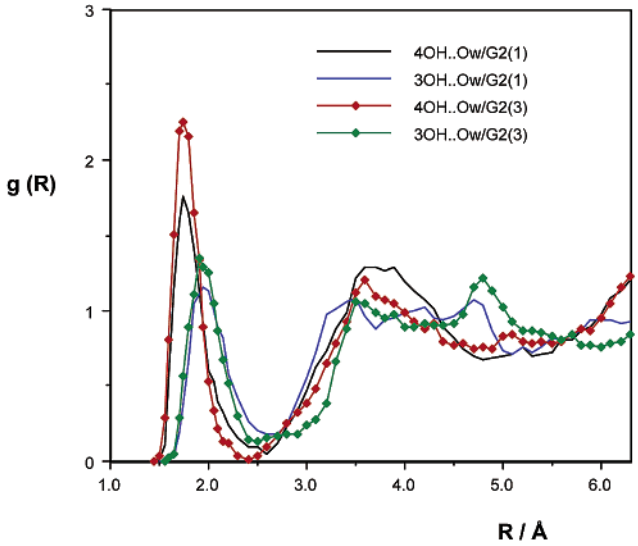

Figure 8. Catechol OH···O_w radial distribution functions, all-atom force field.

(rdf's) until their first minima (Figures 6 and 7) are about 1 (the third NH···O_w rdf is not indicated). The relatively low N_{HB} for G2(3) can also be explained by analysis of the rdf's.

Figure 6 shows the (N)H_t···O_w rdf's characterizing the water−oxygen radial distribution with reference to the trans hydrogen (H−N−C_α–C_β trans) in the NH_3^+ group. H_t is fully exposed to hydration in every conformation; thus, the rdf's are similar. The first peaks are always high and narrow, indicating a well-localized oxygen position in hydration. The second peaks are also well resolved and indicate contributions mainly from localized oxygens hydrating a gauche (N)H atom. (Second-hydration-shell oxygens must be 2.5−3.0 Å away from the first-shell elements and are expected to appear in the rdf's at $R > 4$ Å.) The calculated H_t···O_w coordination numbers are about 1 for all four conformers.

Rdf's for the gauche hydrogens closer to the phenyl ring in the given conformation (H−N−C_α−C_β gauche, Figure 7) show dramatic deviations from the NH_t···O_w rdf's. Coordination numbers for G1(1), T(1), G2(1), and G2(3) are 0.97, 0.99, 0.76, and 0.76, respectively. These gauche hydrogens lean above the phenyl ring in the G2 conformations, and their hydration is partially hindered. Furthermore, not only are the peak values reduced for G2 conformers in Figure 7, but also their shape has changed: the first peaks are remarkably broadened, indicating no strong localization of the water oxygens around these gauche hydrogens of the NH_3^+ group. The other pairs (not shown) of the H_g···O_w rdf's are also different for G2(1) and G(3). Although it is difficult to precisely explain the N_{HB} difference of 0.5 for the two G2 conformers, crossing of pedf's in Figure 5 indicates subtle but important differences in their hydration pattern. Figure 8 confirms this interpretation.

The 4-OH···O_w and 3-OH···O_w rdf's are shown for G2(1) and G2(3) in Figure 8. The peak values are higher both for the 4-OH and 3-OH rdf's in the G2(3) conformation as compared to the G2(1) conformation. A reasonable and consistent reduction of the height of the first maxima was found on going from the 4-OH to the 3-OH rdf's. The O−C_4−C_3−O−H moiety forms a planar, five-membered ring. The hydrogen in the 3-OH group is partially screened from hydration. The (3O)H···O_w coordination numbers are 0.91, 0.70, 1.03, and 0.94 for G1(1), T(1), G2(1), and G2(3), respectively. In T(1), with the conspicuously low coordination number of 0.70, the 3-H atom is out of the plane containing the O_3−C_3−C_4 atoms only by 0.7°. For the other three conformers with coordination numbers of 0.9−1.0, the 3-OH hydrogen out-of-plane torsion angles are 2.9−4.2°. Thus, seemingly very small structural changes lead to noticeable variation in the statistical values calculated for protonated norepinephrine in aqueous solution.

IV. Conclusions

(*R*)-norepinephrine, an important neurotransmitter that activates α- and *β*-adrenergic receptors, takes the monocationic form in 93% concentration at pH 7.4 in aqueous solution. Under these conditions, about 7% of the molecules take either a zwitterionic or the neutral (HO(phenol)···NH_2) form. With respect to its binding to a receptor, the protonated form is the most important as, according to a general view, this protonation state is preserved in the activated receptor−ligand complex. The local conformation of norepinephrine is unknown; thus, in the absence of experimental information, theoretical results are even more valued.

The conformer population for protonated norepinephrine has been found as T(1) > G1(1) > G2(3) > G2(1) at $T = 310$ K and $p = 1$ atm, in fair agreement with the experimental finding at pH 7. The agreement was reached, however, only upon application of a sophisticated approach including in-monohydrate-optimized geometries, consideration of thermal corrections from the monohydrate, using at least MP2/6-31G*//HF/6-31G* internal energies, and applying the all-atom force field in MC/FEP calculations with a small perturbation step size.

Certified by the closeness of the calculated and experimental conformer populations, underlying theoretical structure characteristics may also have significance. The calculated potentials for the rotation of the $-NH_3^+$ group as a single unit about the C_β−C_α axis are largely different in the gas phase (isolated molecule) and in aqueous solution. The 3-fold potential is asymmetric with free energies of barriers in the range of 3.3−11.4 kcal/mol in the gas phase. In contrast, the 2-fold rotational potential of the phenyl ring about the C_1(ring)−C_β axis is nearly symmetrical and hindered by barriers in free energy of 11.1−12.6 kcal/mol. The free energies were calculated using HF/6-31G* results. Energies of barriers calculated at the MP2/6-311++G**//HF/6-31G* level show deviations of 1−2 kcal/mol at most. Free energies of barriers for the $-NH_3^+$ rotation are reduced to 3.7−6.1 kcal/mol in dilute aqueous solution, as calculated by using the united-atom force field. The barriers for the phenyl rotation are reduced only to 8.9−11.9 kcal/mol upon solvation.

The latter finding suggests that a change of the phenyl position to create a better fit between the 3-OH substituent and the neighboring protein side chains is a largely free energy consuming process. This is the case when the T(1) conformer penetrates into the binding pocket of the *β*-adrenergic receptor, and binds there in the T(3) conformation. The gas-phase and in-solution computations may be considered as two systems with opposing dielectric constant extremes. The value relevant in the binding cavity with a limited number of water molecules must be between the extreme values. However, only a high-level and detailed study could explore the dynamics and thermodynamics of the T(1) to T(3) or the G2(3) to T(3) transformations along the penetration route and within the receptor binding pocket.

The sensitivity of the $-NH_3^+$ group rotation to the solvent effect calls attention to the need for a relevant parametrization

of the torsion potentials in molecular mechanics/dynamics calculations. In fact, this is a problem for any molecule with a 1,2-disubstituted aliphatic chain with polar substituents. Atomic charges can change considerably throughout rotation, and formation and disruption of even a strained hydrogen bond is a key element of the free energy change for these molecules upon conformational changes either in their free form or bound to a receptor.

Acknowledgment. P.I.N. is thankful to Professor W. L. Jorgensen for granting him the permission to use the BOSS 3.6 program.

JA028952N